Cerebral Cortex, May 2016;26: 2325–2340

doi: 10.1093/cercor/bhw001
Advance Access Publication Date: 22 February 2016
Original Article

ORIGINAL ARTICLE

Identification of Parvalbumin Interneurons as Cellular Substrate of Fear Memory Persistence

Gürsel Çalışkan[1,2], Iris Müller[2], Marcus Semtner[3], Aline Winkelmann[3,4], Ahsan S. Raza[2], Jan O. Hollnagel[1,5], Anton Rösler[1], Uwe Heinemann[1], Oliver Stork[2,6] and Jochen C. Meier[3,4]

[1]Institute for Neurophysiology, Charité Universitätsmedizin Berlin, Berlin 14195, Germany, [2]Institute of Biology, Department of Genetics and Molecular Neurobiology, Otto-von-Guericke-University, Magdeburg 39120, Germany, [3]Division Cell Physiology, Zoological Institute, Braunschweig 38106, Germany, [4]RNA editing and Hyperexcitability Disorders Helmholtz Group, Max Delbrück Center for Molecular Medicine in the Helmholtz Association, Berlin 13125, Germany, [5]Institute of Physiology and Pathophysiology, University of Heidelberg, Heidelberg 69120, Germany and [6]Center for Behavioral Brain Sciences, Magdeburg, Germany

Address correspondence to Jochen C. Meier, Zoological Institute, Division Cell Physiology, Spielmannstr. 7, 38106 Braunschweig, Germany. Email: jochen.meier@tu-braunschweig.de or to Oliver Stork, Otto-von-Guericke-University, 39120 Magdeburg, Germany. Email: oliver.stork@ovgu.de

Gürsel Çalışkan and Iris Müller contributed equally to this study.

Oliver Stork and Jochen C. Meier contributed equally to this study.

Abstract

Parvalbumin-positive (PV) basket cells provide perisomatic inhibition in the cortex and hippocampus and control generation of memory-related network activity patterns, such as sharp wave ripples (SPW-R). Deterioration of this class of fast-spiking interneurons has been observed in neuropsychiatric disorders and evidence from animal models suggests their involvement in the acquisition and extinction of fear memories. Here, we used mice with neuron type-targeted expression of the presynaptic gain-of-function glycine receptor RNA variant GlyR $\alpha 3L^{185L}$ to genetically enhance the network activity of PV interneurons. These mice showed reduced extinction of contextual fear memory but normal auditory cued fear memory. They furthermore displayed increase of SPW-R activity in area CA3 and CA1 and facilitated propagation of this particular network activity pattern, as determined in ventral hippocampal slice preparations. Individual freezing levels during extinction and SPW-R propagation were correlated across genotypes. The same was true for parvalbumin immunoreactivity in the ventral hippocampus, which was generally augmented in the GlyR mutant mice and correlated with individual freezing levels. Together, these results identify PV interneurons as critical cellular substrate of fear memory persistence and associated SPW-R activity in the hippocampus. Our findings may be relevant for the identification and characterization of physiological correlates for posttraumatic stress and anxiety disorders.

Key words: contextual fear memory, hippocampus, interneurons, memory extinction, parvalbumin, sharp wave ripples

© The Author 2016. Published by Oxford University Press.
This is an Open Access article distributed under the terms of the Creative Commons Attribution Non-Commercial License (http://creativecommons.org/licenses/by-nc/4.0/), which permits non-commercial re-use, distribution, and reproduction in any medium, provided the original work is properly cited. For commercial re-use, please contact journals.permissions@oup.com

Introduction

The hippocampal formation is involved in diverse behaviors such as stress-adaptive responding (McEwen 2012), spatial orientation (Buzsaki and Moser 2013), and explicit memory (Pilly and Grossberg 2012; Buzsaki and Moser 2013). In particular, significant progress has been made regarding the neuronal mechanisms in the hippocampus that underlie the formation and retrieval of contextual fear memory (Lovett-Barron et al. 2014). Recent evidence reveals a decisive role of parvalbumin-positive (PV) hippocampal interneurons in contextual fear learning (Donato et al. 2013, 2015). PV neurons provide perisomatic inhibition to hippocampal principle cells and are critically involved in the generation and propagation of behavior-related network activity patterns in the hippocampus (Gulyas et al. 2010; Hajos et al. 2013; Hu et al. 2014; Schlingloff et al. 2014). Their distribution shows a clear dorsoventral gradient with high numbers in the ventral hippocampus (Caballero et al. 2013). Moreover, ventral hippocampal PV neurons are less strongly upregulated upon chronic stress exposure (Czeh et al. 2015) but more responsive to redox stress (Steullet et al. 2010), indicating an important contribution of these interneurons to the functional divergence of the hippocampus along its dorso-ventral axis. However, how the network activity patterns that are generated and transported by the PV neurons contribute to the function of hippocampal subregions is still not sufficiently understood.

We recently presented mice with targeted expression of glycine receptor (GlyR) RNA variant $\alpha3L^{185L}$ in presynaptic terminals of PV interneurons. Our animal model with PV interneuron-targeted expression of the gain-of-function GlyR RNA variant $\alpha3L^{185L}$ (Winkelmann et al. 2014) is based on previous observations that GlyR $\alpha3L^{185L}$ expression is increased in hippocampectomies of patients with mesial temporal lobe epilepsy (mTLE) (Eichler et al. 2008; Legendre et al. 2009). Targeted expression of this gain-of-function GlyR variant facilitates presynaptic release of the neurotransmitter GABA and thereby strengthens the weight of PV interneurons in the neural network, providing a powerful animal model for genetically enhanced network function of this particular type of interneuron and investigation of the role of PV interneurons with regard to neuropsychiatric comorbidity of epilepsy (Winkelmann et al. 2014). In this recent study $Hprt^{\alpha3L185L\ +/0}$; $Pvalb^{Cre\ +/-}$ mice showed unaltered spatial reference memory, which is thought to depend specifically on dorsal hippocampus, but presented with increased anxiety (Winkelmann et al. 2014), indicating a potential change in the function of ventral hippocampus and/or amygdala function (Bannerman et al. 2004). Therefore, in the current study, we investigated the formation and extinction of contextual fear memory, which are known to depend, particularly, on the function of the ventral hippocampus (Rudy and Matus-Amat 2005; Rosas-Vidal et al. 2014), as well as associated PV-interneuron dependent network activity patterns in $Hprt^{\alpha3L185L+/0}$; $Pvalb^{Cre\ +/-}$ mice.

Explicit memories, including context representations, are not stored permanently in the hippocampus but require transfer of information from the hippocampus to the cortical mantle (Buzsaki 1989; Battaglia et al. 2011). This process is facilitated by replay of previously stored information in compressed form during sharp wave-ripple complexes (SPW-Rs) (Buzsaki et al. 1992; Wilson and McNaughton 1994; Nadasdy et al. 1999). SPW-Rs are 30 to 80-ms field potential transients, which are superimposed by ripples with a frequency of about 200 Hz (Buzsaki et al. 1992; Maier et al. 2003, 2009). They occur during quiescent behavior and slow-wave sleep (Suzuki and Smith 1988; Buzsaki 1989; Nakashiba et al. 2009), which supports consolidation of explicit memories in humans (Marshall et al. 2006; Rasch et al. 2007). They also appear in hippocampal slice preparations of mice as spontaneous events which often originate from area CA3 and propagate to area CA1, the subiculum and eventually from there into the cortical mantle (Chrobak and Buzsaki 1996; Maier et al. 2003). PV interneurons are central elements in the generation of SPW-R in the hippocampus (Hajos et al. 2013; Schlingloff et al. 2014). Thus, we reasoned that persistent fear memory storage of $Hprt^{\alpha3L185L\ +/0}$; $Pvalb^{Cre\ +/-}$ mice might be associated with alterations in memory consolidation-related processes supported by hippocampal SPW-R activity. Indeed, our data demonstrate facilitated SPW-R transfer between hippocampal CA3 and CA1 regions as a critical network characteristic of these animals.

Materials and Methods

Animals

Animals were handled according to permits (T0122/07; T0212/08; and O-0389/10) given by the Office for Health Protection and Technical Safety of the regional council of Berlin (LaGeSo) and in compliance with regulations laid down in the European Community Council Directive. As described recently (Winkelmann et al. 2014) GlyR $\alpha3L^{185L}$ expression in PV interneurons was achieved by mating homozygous B6;129P2-*Hprt*<tm1(CAG-Glra3*)Jcme (MGI ID: 5608589, abbreviated: $Hprt^{\alpha3L185L\ +/+}$) females with homozygous B6;129P2-*Pvalb*<tm1(cre)Arbr>/J (MGI ID: 3590684, abbreviated: $Pvalb^{Cre\ +/+}$) males (Jackson Laboratories, USA). Sibling males and sibling females were used for parallel mutant and control breeding to minimize genetic background variation. Adult male offspring ($Hprt^{\alpha3L185L\ +/0}$; $Pvalb^{Cre\ +/-}$), hemizygous for the GlyR $\alpha3L^{185L}$ allele and heterozygous for the $Pvalb^{Cre}$ allele aged 3–12 months were used in all experiments. Age-matched $Hprt^{\alpha3L185L\ +/0}$ male mice were used as control animals. A second control group comprised of $Hprt^{\alpha3L185L\ +/0}$; $Camk2a^{Cre\ +/-}$ mice was derived from breeding of $Hprt^{\alpha3L185L\ +/+}$ females with heterozygous B6.FVB-Tg(*Camk2a*-cre)2Gsc/Cnrm (MGI ID:2181426, abbreviated: $Camk2a^{Cre\ +/-}$) males (Casanova et al. 2001) (kindly provided by Günther Schütz, German Cancer Research Center DKFZ, Heidelberg, Germany). In our previous study, we confirmed that GlyR $\alpha3L^{185L}$ is expressed in all hippocampal sectors (DG, CA3, and CA1) at presynaptic termini of glutamatergic synapses using electron microscopy, and of PV interneuron synapses using confocal microscopy (Winkelmann et al. 2014). Behavioral, electrophysiological, and immunohistochemical experiments were performed blind to genotype.

Behavior

Mice ($N = 7$ $Hprt^{\alpha3L185L\ +/0}$; $Pvalb^{Cre\ +/-}$, $N = 10$ $Hprt^{\alpha3L185L\ +/0}$ controls) were first analyzed in the hot plate test (see Supplementary Methods) to rule out a priori differences in pain sensitivity (measured by latency to lick hind paws) and 3 weeks later trained in a contextual fear conditioning/fear extinction task. Training was done in a fear conditioning apparatus (TSE Bad Homburg, Germany) under low illumination (10 lux). Three daily 2.5-min training sessions were applied with each one unsignaled electric foot shock (1 s, 0.4 mA). Fear extinction was analyzed in 5 daily 10 min sessions of exposure to the training context without footshock reinforcement. Fear behavior (complete immobility except for respiratory movements, measured in the number of freezing bouts and the freezing duration expressed as % of the test interval), was rigorously evaluated in 2 min bins throughout the task (see Supplementary Methods). Moreover, exploratory activity with a

velocity between 3 cm/s and 20 cm/s was determined to measure nondefensive behavioral activity during habituation. Freezing and activity levels were in general agreement with our previous observations (e.g., Albrecht et al, 2010; Sangha et al. 2009) and thus allowed us to address both potential increase and decrease of performance during training and extinction.

In this first behavioral experiment an additional group of $Hprt^{\alpha 3L185L\ +/0}$; $Camk2a^{Cre\ +/-}$ mice ($N = 9$) from the same breeding was included as additional controls (Winkelmann et al. 2014), in order to control for the cell-type specificity of observed effects.

A second batch of $Hprt^{\alpha 3L185L\ +/0}$; $Pvalb^{Cre\ +/-}$ mice ($N = 10$) and $Hprt^{\alpha 3L185L\ +/0}$ control mice ($N = 9$) was trained in an auditory cued fear conditioning and extinction paradigm (see Supplementary Methods). To allow for a close comparison with contextual memory, freezing levels were analyzed during tone intervals in 2 min bins (i.e., as average of % time or sum of bouts over each 4 tones per 2 min).

A third batch of animals ($Hprt^{\alpha 3L185L\ +/0}$; $Pvalb^{Cre\ +/-}$ mice, $N = 8$; $Hprt^{\alpha 3L185L\ +/0}$ control mice, $N = 8$) was used to obtain individual correlation between the freezing level of the mouse with SPW-R activity. Here context-dependent memory was tested similar to the first set of experiments, but mice were sacrificed 1 h after the E2 session and horizontal slices were obtained from the ventral hippocampus of the corresponding mouse (see Supplementary Methods). Since the behavioral difference was strongest at the initial phase of each extinction session, E2, here, was limited to only 2 min. For calculation of correlation to freezing behavior the average SPW-R values of 2–5 slices per mice were used. Only slices exhibiting SPW-Rs in both CA3 and CA1 were further processed for correlation analysis.

Electrophysiology

Horizontal brain slices from ventral hippocampus were prepared as described earlier (Albrecht et al. 2013) and local field potential (LFP) recordings were obtained from CA3 and CA1 pyramidal layer (see Supplementary Methods and Supplementary Fig. 1). Characteristics of SPW-R activity and CA3–CA1 network interactions were analyzed using a MATLAB-based code (MathWorks, Natick, MA; see Supplementary Methods).

To find out whether SPW-R can be recorded in isolated slices of the dorsal hippocampus, transverse-like slices of the dorsal hippocampus from naïve C57BL/6 mice were obtained using several methods described in the literature (Papatheodoropoulos and Kostopoulos 2000, 2002; Steullet et al. 2010; Dougherty et al. 2012; see also Supplementary Methods).

Immunohistochemical Analysis of Parvalbumin Immunoreactivity

Another batch of $Hprt^{\alpha 3L185L\ +/0}$; $Pvalb^{Cre\ +/-}$ mice ($N = 7$) and $Hprt^{\alpha 3L185L\ +/0}$ control mice ($N = 5$) were trained in a contextual fear conditioning and extinction paradigm as described above. Again, in order to avoid a potentially confounding effect of within-session habituation of freezing E2 was limited to only 2 min, and mice were sacrificed 1 h thereafter. Mice were anesthetized with Pentobarbital (i.p., 50 mg/kg) and preperfused with 0.9% NaCl (ca. 30 mL). After complete blood wash out, animals were perfused with 4% paraformaldehyde (PFA, ca. 100 mL) and brains were then transferred to 4% PFA overnight (at 4°C). One day later brains were transferred to 30% sucrose and 0.02% NaN_3 for the purpose of cryoprotection. From each animal, cryosections (25 µm) were obtained in coronal and horizontal planes (CM1850, Leica Microsystems, Wetzlar, Germany) for investigation of dorsal and ventral hippocampi, respectively, and mounted on Superfrost Plus microscope slides (Menzel GmbH, Braunschweig, Germany). Dorsal and ventral hippocampi were set at –2.1 mm and –4.56 mm, respectively, from bregma. Sections were stained with an anti-parvalbumin mouse monoclonal antibody (clone 235, 1:2500; Swant), as described recently (Winkelmann et al. 2014) and visualized using carboxymethyl indocyanine- (Cy5-) conjugated secondary antibody (Jackson Immunoresearch Laboratories, USA). Cell nuclei were stained with DAPI.

Confocal images were acquired with an inverted confocal laser scanning microscope LSM700 (Zeiss) equipped with a 20× NA 0.8 PlanApochromat objective. Z-stacks and tile scans were acquired with 0.5 µm lateral and 4 µm axial pixel size to identify individual nuclei and cells. A 405 nm laser (set at 1.2% of 5 mW) was used for excitation and SP490 filter for detection of DAPI. A 639 nm laser (5 mW) and LP640 filter was used for detection of parvalbumin (Cy5). To exploit the full dynamic range (12 bit) of the parvalbumin signals the 639 nm laser power was changed for individual slices in a way that <20% of the pixels belonging to the brightest PV cells were saturated, referring to experiments described recently (Donato et al. 2013). However, in contrast to the elegant study by Donato et al. (2013), changing laser power was necessary here in our semiquantitative analysis because the immunochemical analysis of parvalbumin signal intensity was performed blind with regard to genotype and freezing duration. Thus, due to the experimental procedure, there was no "control" animal group for optimization of laser power and use of constant laser settings throughout the experiment, but Supplementary Figure 2 shows that, even though changing laser power, there was no correlation between background signal intensity (calculated from the whole CA3b region outside of the ROIs and given as the average fluorescence of the maximum intensity z-projection) and freezing duration. The fluorescence signal of PV cells was quantified using a procedure written in IGOR 6.3 (WaveMetrics, USA). PV cells were identified manually by selecting regions of interest (ROIs, 15 × 15 µm) in the respective CA3 region of each z-section. Parvalbumin signals not associated with a cell nucleus were excluded from analysis. Background fluorescence was subtracted. Subsequent quantification of the parvalbumin signal intensities was done by averaging the fluorescence signal of each ROI using the bit values of the maximum intensity z-projection. The threshold to distinguish between PV cells with different parvalbumin signal intensities was set for each slice separately by setting the respective background fluorescence value to 0% and the fluorescence value from the maximum PV cell to 100%. Classification was done using the following thresholds: 0–25% (low), 25–50% (intermediate low), 50–75% (intermediate high), and 75–100% (high). Then, the proportions in percent of PV cells with low, intermediate low, intermediate high, or high parvalbumin signal intensities was calculated and averaged (3–5 slices per animal and ventral or dorsal hippocampus). These values were further used for analysis of correlation with individual freezing durations at E2.

Statistics and Data Presentation

Statistical analysis and data presentation were performed using SigmaPlot (Systat Software Inc.) and SPSS 22.0 (IBM Germany GmbH, Ehningen, Germany) for analysis of the behavior data. Accordingly, one-way ANOVA or Kruskal–Wallis one-way analysis of variance on ranks was used to assess differences between the groups. One-way ANOVA was applied for the hot plate test and percent activity at T1 before first shock presentation, repeated-measures ANOVA for fear conditioning and extinction.

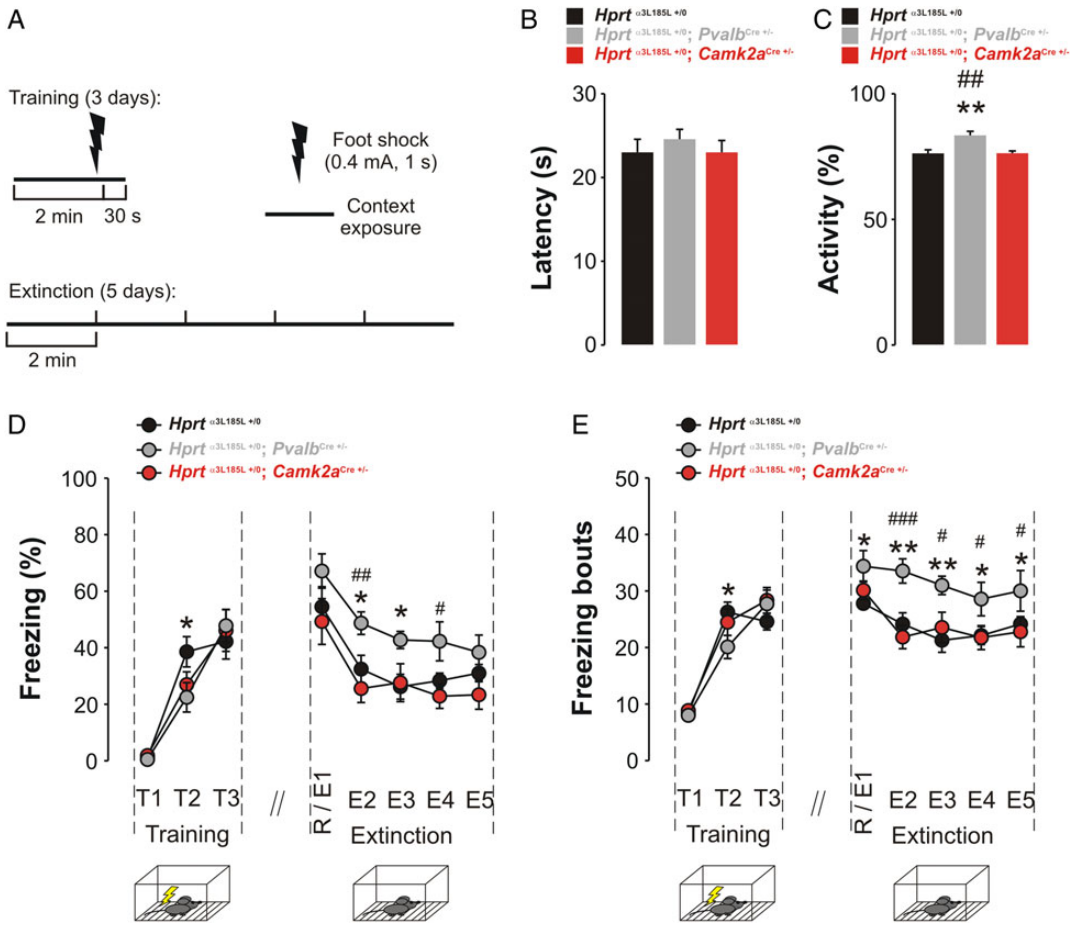

Figure 1. Fear extinction is impaired in mice with enhanced functionality of PV interneurons ($Hprt^{\alpha 3L185L\ +/0}$; $Pvalb^{Cre\ +/-}$). (*A*) Sketch of the fear conditioning protocol. Mice received 3 consecutive daily training and 5 consecutive daily extinction sessions. Memory performance was analyzed in 2 min bins. (*B*) A hot plate test confirmed an equal pain threshold in all 3 genotypes, as measured by latency to lick hind paws (black bar: $Hprt^{\alpha 3L185L\ +/0}$ (control), gray bar: $Hprt^{\alpha 3L185L\ +/0}$; $Pvalb^{Cre\ +/-}$, red bar: $Hprt^{\alpha 3L185L\ +/0}$; $Camk2a^{Cre\ +/-}$). (*C*) Baseline exploratory activity before first shock presentation. $Hprt^{\alpha 3L185L\ +/0}$; $Pvalb^{Cre\ +/-}$ mice were more active than mice in the other 2 groups (black bar: $Hprt^{\alpha 3L185L\ +/0}$ (control), gray bar: $Hprt^{\alpha 3L185L\ +/0}$; $Pvalb^{Cre\ +/-}$, red bar: $Hprt^{\alpha 3L185L\ +/0}$; $Camk2a^{Cre\ +/-}$). (*D*) Freezing duration in percent time of the first 2 min of each session is displayed as a measure of long-term fear memory. A mild reduction in freezing was observed in $Hprt^{\alpha 3L185L\ +/0}$; $Pvalb^{Cre\ +/-}$ mice at training day T2, but genotypes performed equally upon further training. During extinction $Hprt^{\alpha 3L185L\ +/0}$; $Pvalb^{Cre\ +/-}$ mice showed consistently higher freezing levels than $Hprt^{\alpha 3L185L\ +/0}$ (control) and $Hprt^{\alpha 3L185L\ +/0}$; $Camk2a^{Cre\ +/-}$ mice. (*E*) Number of freezing bouts in the first 2 min of each session is displayed. Similar to the freezing duration, the number of freezing bouts was reduced in the $Hprt^{\alpha 3L185L\ +/0}$; $Pvalb^{Cre\ +/-}$ group at T2. Moreover, bouts were increased at R/E1 and remained high throughout extinction. Data represent mean ± SEM. T1–T3 = training days 1–3, R = retrieval, E1–5 = extinction days 1–5. Significant difference between $Hprt^{\alpha 3L185L\ +/0}$ and $Hprt^{\alpha 3L185L\ +/0}$; $Pvalb^{Cre+/-}$ mice is indicated with asterisks. Significant difference between $Hprt^{\alpha 3L185L\ +/0}$; $Camk2a^{Cre\ +/-}$ and $Hprt^{\alpha 3L185L\ +/0}$; $Pvalb^{Cre\ +/-}$ mice is indicated using #, ##, or ### symbols. (*,#: $P < 0.05$; **,##: $P < 0.01$; ***, ###: $P < 0.001$).

If applicable, Fisher's LSD test was performed for post hoc comparisons. Electrophysiological data were evaluated for normality (Shapiro–Wilk Test) and equal variance before assessing statistical significance of mean values. Then, either Student's *t*-test or Mann–Whitney *U* test was used to compare genotype effect. For analysis of consolidation of extinguished fear memory between extinction sessions, dependent samples *t*-test was performed. Pearson Product Moment Correlation was used to assess the correlation between 2 parameters. *P* values below 0.05 were considered significant.

Results

Impaired Extinction of Context Fear Memory

Considering the established role of PV hippocampal interneurons in contextual fear learning and anxiety-related behavior (Donato et al. 2013; Winkelmann et al. 2014), we tested acquisition and extinction of hippocampus-dependent contextual fear memory in $Hprt^{\alpha 3L185L\ +/0}$; $Pvalb^{Cre\ +/-}$ mice (Fig. 1A). $Hprt^{\alpha 3L185L\ +/0}$ mice were used as controls and an additional group of $Hprt^{\alpha 3L185L\ +/0}$; $Camk2a^{Cre\ +/-}$ was included to the analysis to confirm cell-type specificity of effects (Winkelmann et al. 2014).

Before conditioning, we controlled for potential confounds that might affect stimulus evaluation or expression of conditioned fear. A comparable pain threshold in all 3 genotypes was confirmed in the hot plate test measured by latency to lick hind paws (Fig. 1B; $F_{2,23} = 0.346$, $P > 0.05$). Altered exploratory activity became evident during the pretraining exposure to the training context (one-way ANOVA, $F_{2,23} = 8.839$, $P < 0.01$) due to $Hprt^{\alpha 3L185L\ +/0}$; $Pvalb^{Cre\ +/-}$ mice showing more activity than the other 2 genotypes ($P < 0.01$, Fisher's LSD test; Fig. 1C). However, pretraining incidence of freezing duration and number of freezing bouts at the first day of training (T1) were comparable between genotypes (Fig. 1D,E).

In addition to freezing and exploratory activity, behaviors involving slow or small movements such as alert watching, stretched attending or grooming were displayed by the experimental animals at low frequency and with high interindividual

difference, in agreement with our previous observations (Laxmi et al. 2003). These behaviors were not further considered for the analysis of fear memory.

To test the acquisition and stability of long-term fear memory, freezing behavior was determined during the first 2 min of each fear conditioning and fear extinction session (Fig. 1*D*,*E*). As described earlier, we binned the data in 2 min to decode any time-dependent between-session and within-session effects in a most accurate manner possible (Sangha et al. 2009). Significant session effects became evident concerning both the freezing duration (repeated-measures ANOVA, $F_{7,161} = 58.714$, $P < 0.001$; Fig. 1*D*) and the number of freezing bouts ($F_{7,161} = 58.708$, $P < 0.001$; Fig. 1*E*) as freezing levels generally increased during training and decreased during extinction. In the absence of a significant main effect of genotype, we further observed significant interactions of session and genotype for both fear measures (freezing duration: $F_{14,161} = 3.161$, $P < 0.01$, Fig. 1*D*; freezing bouts: $F_{14,161} = 4.313$, $P < 0.001$, Fig. 1*E*). Across the 3 training sessions, both freezing duration and the number of freezing bouts increased in all genotypes (T1 vs. T3: $P < 0.001$, Fischer's LSD, Fig. 1*D*,*E*). *Hprt*$^{\alpha 3L185L\ +/0}$; *Pvalb*$^{Cre\ +/-}$ showed a slow acquisition of the task with reduced freezing duration after the first training day ($P < 0.05$ compared with *Hprt*$^{\alpha 3L185L\ +/0}$ control mice), but this difference was fully overcome in the following training sessions.

In contrast, fear extinction proved to be strictly dependent on genotype. *Hprt*$^{\alpha 3L185L\ +/0}$; *Pvalb*$^{Cre\ +/-}$ mice displayed consistently higher freezing levels than *Hprt*$^{\alpha 3L185L\ +/0}$ controls (freezing duration E2, E3: $P < 0.05$; freezing bouts R/E1–E5: $P < 0.05$; for details see diagram Fig. 1*D*,*E*). In fact, *Hprt*$^{\alpha 3L185L\ +/0}$; *Pvalb*$^{Cre\ +/-}$ mice showed less reduction in freezing duration and in contrast to controls (*Hprt*$^{\alpha 3L185L\ +/0}$ E3, E4: $P < 0.05$; *Hprt*$^{\alpha 3L185L\ +/0}$; *Camk2a*$^{Cre\ +/-}$ E2, E4, E5: $P < 0.01$, E3: $P < 0.05$) entirely failed to reduce the number of freezing bouts compared with their first memory retrieval session. *Hprt*$^{\alpha 3L185L\ +/0}$ *and Hprt*$^{\alpha 3L185L\ +/0}$; *Camk2a*$^{Cre\ +/-}$ mice did not differ from each other during either acquisition or extinction of fear memory.

Extinction: Within-session Freezing Response

As the next step, we analyzed the decline of the freezing response within each extinction session across five 2-min intervals (i1–i5, Fig. 2).

In the retrieval and first extinction training session R/E1 (Fig. 2*A*), a significant main effect for the interval was observed ($F_{4,92} = 21.388$, $P < 0.001$), but no effect of the genotype ($F_{2,23} = 0.739$, $P > 0.05$) or a genotype × interval interaction ($F_{8,92} = 1.649$, $P > 0.05$) was detected. Post hoc comparison revealed a reduction of freezing compared with the first interval i1 in all 3 genotypes (*Hprt*$^{\alpha 3L185L\ +/0}$: i3–i5 vs. i1: $P < 0.05$; *Hprt*$^{\alpha 3L185L\ +/0}$; *Camk2a*$^{Cre\ +/-}$: i3, i4 vs. i1: $P < 0.05$; *Hprt*$^{\alpha 3L185L\ +/0}$; *Pvalb*$^{Cre\ +/-}$: i4, i5 vs. i1: $P < 0.01$).

In session E2 (Fig. 2*B*), a significant effect was evident for the interval ($F_{4,92} = 7.964$, $P < 0.001$) as well as for genotype × interval interaction ($F_{8,92} = 3.043$, $P < 0.01$), but no significant effect for the genotype alone ($F_{2,23} = 3.168$, $P > 0.05$) was observed. *Hprt*$^{\alpha 3L185L\ +/0}$ mice reduced the time spent freezing from the first to the fourth interval ($P < 0.05$). However, *Hprt*$^{\alpha 3L185L\ +/0}$; *Pvalb*$^{Cre\ +/-}$ mice displayed high freezing levels in the beginning, which declined during each session (i3: $P < 0.05$, i4: $P < 0.001$, i5: $P < 0.01$; i3 vs. i2: $P < 0.05$, i4 vs. i2: $P < 0.001$, i5 vs. i2: $P < 0.01$). *Hprt*$^{\alpha 3L185L\ +/0}$; *Camk2a*$^{Cre\ +/-}$ showed no significant changes between intervals.

A similar pattern emerged in E3 (Fig. 2*C*) with *Hprt*$^{\alpha 3L185L\ +/0}$; *Pvalb*$^{Cre\ +/-}$ mice showing high freezing levels in i1 and i2 and alignment with the other 2 genotypes during i3–i5. Thus a significant interval effect ($F_{4,92} = 9.278$, $P < 0.001$) and a significant genotype × interval interaction ($F_{8,92} = 3.857$, $P < 0.01$) but no main genotype effect emerged ($F_{2,\ 23} = 1.509$, $P > 0.05$). Pair-wise comparisons confirmed a significant reduction from the first 2 intervals to the last 3 in *Hprt*$^{\alpha 3L185L\ +/0}$; *Pvalb*$^{Cre\ +/-}$ mice only (i3–5 vs. i1: $P < 0.01$, i3–5 vs. i2: $P < 0.01$).

The same pattern was observed in session E4 (Fig. 2*D*) with a significant interval effect ($F_{4,92} = 4.487$, $P < 0.01$) and a significant interaction ($F_{8,92} = 3.49$, $P < 0.01$) but no genotype effect ($F_{2,23} = 0.59$, $P > 0.05$). Again, freezing diminished only in *Hprt*$^{\alpha 3L185L\ +/0}$; *Pvalb*$^{Cre\ +/-}$ mice during the session (i1 vs. i4, i5: $P < 0.01$; i2 vs. i4, i5: $P < 0.05$; i3 vs. i5: $P < 0.05$).

Finally, for session E5 (Fig. 2*E*) a significant interval effect ($F_{4,92} = 5.972$, $P < 0.001$) and a significant interaction ($F_{8,92} = 2.409$, $P < 0.05$) arose. The genotype alone did not yield a significant effect ($F_{2,23} = 0.016$, $P > 0.05$). In the *Hprt*$^{\alpha 3L185L\ +/0}$; *Pvalb*$^{Cre\ +/-}$ mice the first interval i1 differed significantly from each i3, i4, and i5 ($P < 0.05$), and the i2 differed from i4 ($P < 0.05$). Again, no significant habituation was found in the other groups.

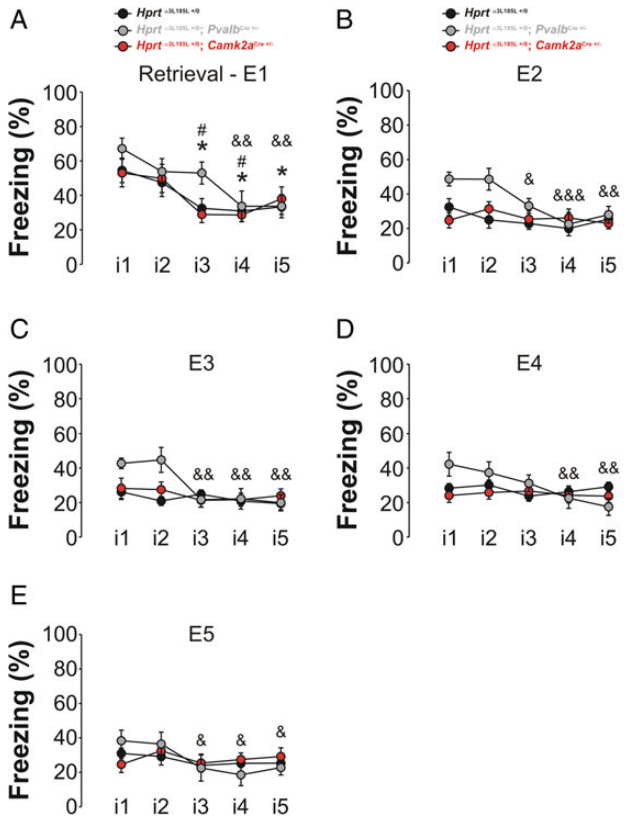

Figure 2. Altered within-session fear extinction in *Hprt*$^{\alpha 3L185L\ +/0}$; *Pvalb*$^{Cre\ +/-}$ mice. For a detailed analysis of freezing behavior within extinction sessions, each five 2-min intervals (i1–i5) were analyzed. *Hprt*$^{\alpha 3L185L\ +/0}$; *Pvalb*$^{Cre\ +/-}$ mice showed high initial freezing levels and significant decline during each session: E1–-Retrieval (*A*), E2–Extinction Day 2 (*B*), E3–Extinction Day 3 (*C*), E4–Extinction Day 4 (*D*), E5–Extinction Day 5 (*E*). *Hprt*$^{\alpha 3L185L+/0}$ and *Hprt*$^{\alpha 3L185L\ +/0}$; *Camk2a*$^{Cre\ +/-}$ mice showed within-session extinction only during E1 and displayed constantly low freezing levels thereafter. (black label: *Hprt*$^{\alpha 3L185L\ +/0}$ (control), gray label: *Hprt*$^{\alpha 3L185L\ +/0}$; *Pvalb*$^{Cre\ +/-}$, red label: *Hprt*$^{\alpha 3L185L\ +/0}$; *Camk2a*$^{Cre\ +/-}$). Data represent mean ± SEM and are reported as percent time of the investigated 2-min time interval. Asterisks (*) indicate significant differences to the first interval within *Hprt*$^{\alpha 3L185L\ +/0}$ genotype. The "&" symbol indicates significant difference to the first interval within *Hprt*$^{\alpha 3L185L\ +/0}$; *Pvalb*$^{Cre\ +/-}$ genotype, $P < 0.05$; &&, $P < 0.01$; &&&, $P < 0.001$. "#" indicates significant differences to the first interval within *Hprt*$^{\alpha 3L185L\ +/0}$; *Camk2a*$^{Cre\ +/-}$ genotype, $P < 0.05$.

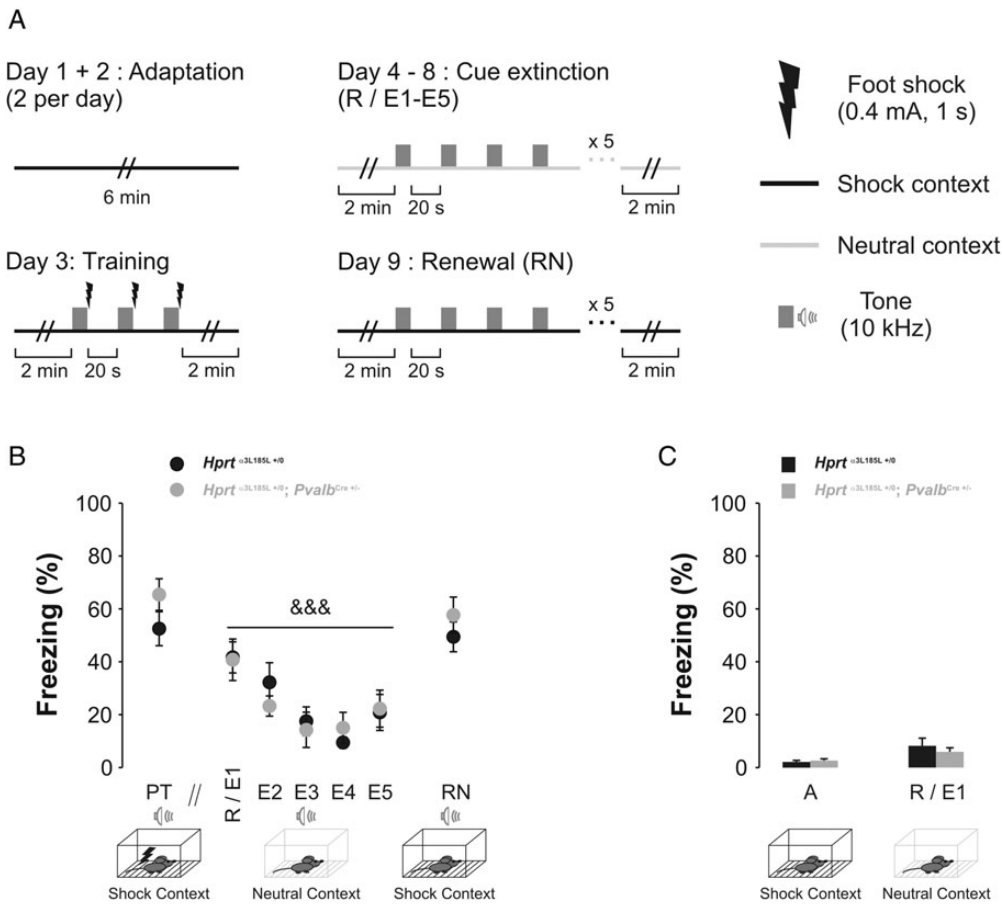

Figure 3. Auditory cued fear conditioning and extinction are unaltered in mice with enhanced functionality of PV interneurons ($Hprt^{\alpha 3L185L\ +/0}$; $Pvalb^{Cre\ +/-}$). (*A*) Sketch of the conditioning protocol. Mice received a total of 4 adaptation sessions to the background context. Conditioning to a tone was performed in 3 tone–shock pairings, followed by extinction of the tone fear memory in a neutral context on 5 consecutive days. Finally, renewal (context-dependency of an extinguished fear response) was tested by presenting the tone in the shock context. (*B*) Both genotypes displayed comparable post training freezing, auditory fear memory extinction and fear renewal in the original shock context. (*C*) Likewise, genotypes did not differ in pretraining shock context or pre-extinction neutral context freezing. Contextual freezing levels in (*B*) and (*C*) are reported in percent time of 2 min, cued freezing in percent time of the first 4 10-s stimulus presentations of each session (distributed over 2 min). Data are mean ± SEM. R = retrieval, E1–E5 = extinction days 1–5, RN = renewal, PT = post training, A = adaptation. &&& indicate a significant main effect for extinction sessions $P < 0.001$.

Failure in Consolidation of Fear Extinction

Based on the observed deficit in long-term contextual extinction memory and acute habituation during each extinction session with high initial freezing levels in $Hprt^{\alpha 3L185L\ +/0}$; $Pvalb^{Cre\ +/-}$ mice, we further analyzed the consolidation of extinguished fear memory between daily sessions. To this end, we compared the last 2-min interval of each extinction session E1–E4 with the first 2-min interval of the following ones Supplementary Figure 3). A deficit to consolidate fear extinction was observed only in $Hprt^{\alpha 3L185L\ +/0}$; $Pvalb^{Cre\ +/-}$ mice but not in any other group (freezing duration in $Hprt^{\alpha 3L185L\ +/0}$; $Pvalb^{Cre\ +/-}$: R/E1 vs. E2: $t_{(6)} = -2.122$, $P > 0.05$; E2 vs. E3: $t_{(6)} = -2.501$, $P < 0.05$; E3 vs. E4: $t_{(6)} = -3.329$, $P < 0.05$; E4 vs. E5: $t_{(6)} = -5.202$, $P < 0.01$; freezing bouts: R/E1 vs. E2: $t_{(6)} = -4.727$, $P < 0.01$; E2 vs. E3: $t_{(6)} = -3.107$, $P < 0.05$; E3 vs. E4: $t_{(6)} = -3.359$, $P < 0.05$; E4 vs. E5: $t_{(6)} = -5.31$, $P < 0.01$).

To sum up, detailed analysis of each extinction session reveals that while freezing levels in both other groups declined only in the first session and remained low thereafter, $Hprt^{\alpha 3L185L\ +/0}$; $Pvalb^{Cre\ +/-}$ mice freezing levels habituated acutely during each extinction session and then recovered overnight initial high levels to the next session.

Unaltered Auditory Cued Fear Memory

To test whether the observed extinction deficit was specific for contextual fear memory, we performed auditory cued fear memory with control ($Hprt^{\alpha 3L185L\ +/0}$) and $Hprt^{\alpha 3L185L\ +/0}$; $Pvalb^{Cre\ +/-}$ mice (Fig. 3A). Here, neither conditioning nor extinction were significantly altered in $Hprt^{\alpha 3L185L\ +/0}$; $Pvalb^{Cre\ +/-}$ mice (Fig. 3B). Both genotypes displayed a significant decline of freezing over the course of the 5 extinction sessions (repeated-measurement ANOVA for freezing duration: session effect: $F_{4,68} = 12.141$, $P < 0.001$, session × genotype effect: $F_{4,68} = 0.683$, $P = 0 > 0.05$, genotype effect: $F_{1,17} = 0.034$, $P > 0.05$; repeated-measures ANOVA for number of freezing bouts: session effect: $F_{4,68} = 10.536$, $P < 0.001$, session × genotype effect: $F_{4,68} = 0.642$, $P > 0.05$, genotype: $F_{1,17} = 0.164$, $P > 0.05$). Moreover, fear responses were comparable when the tone was presented in the shock context (renewal: *t*-test for freezing duration: $t_{(17)} = 0.442$, $P > 0.05$; *t*-test for number of freezing bouts: $t_{(17)} = 1.811$, $P > 0.05$; Figure 3B).

Mice responded similarly to the first shock context presentation before training (*t*-test for freezing duration: $t_{(17)} = -0.568$, $P > 0.05$; *t*-test for number of freezing bouts: $t_{(17)} = -1.42$, $P > 0.05$), as well as immediately thereafter (*t*-test for freezing duration:

$t_{(17)} = -1.473$, $P > 0.05$; *t*-test for number of freezing bouts: $t_{(17)} = 1.634$, $P > 0.05$), and to the first presentation of the neutral context before extinction (*t*-test for freezing duration: $t_{(17)} = 0.705$, $P > 0.05$; *t*-test for number of freezing bouts: $t_{(17)} = -0.41$, $P > 0.05$; Figure 3C). Moreover, there were no differences between genotypes in the first 2-min bin of the first adaptation and the last 2 min of the last adaptation, and both control and *Hprt*$^{\alpha 3L185L\ +/0}$; *Pvalb*$^{Cre\ +/-}$ mice thus habituated similarly to a so-far neutral context ($P \geq 0.05$, data not shown). Cumulatively, these results identify a specific impairment of contextual fear memory extinction in *Hprt*$^{\alpha 3L185L\ +/0}$; *Pvalb*$^{Cre\ +/-}$ mice.

Enhanced Hippocampal Sharp Wave-ripples in *Hprt*$^{\alpha 3L185L\ +/0}$; *Pvalb*$^{Cre\ +/-}$ mice

We hypothesized that the lack of extinction consolidation in *Hprt*$^{\alpha 3L185L\ +/0}$; *Pvalb*$^{Cre\ +/-}$ mice might be related to a role of PV interneurons in controlling hippocampal network activity patterns. In particular, PV neurons are involved in sharp wave-ripple (SPW-R) activity (Hajos et al. 2013; Hu et al. 2014; Schlingloff et al. 2014), which is crucial for memory consolidation (Girardeau et al. 2009; Nakashiba et al. 2009).

Therefore, we performed extracellular field potential recordings in area CA3 and CA1 of horizontal hippocampal slices from *Hprt*$^{\alpha 3L185L\ +/0}$; *Pvalb*$^{Cre\ +/-}$ mice. SPW-Rs resembling those recorded in vivo (Csicsvari et al. 1999; Maier et al. 2012) were detected in the majority (127 out of 180) of the investigated slice preparations from the ventral hippocampus (Supplementary Figs 1, 3 and Fig. 4A,B). In contrast, in spite of systematic methodological development we, like others (Papatheodoropoulos and Kostopoulos 2002), were not able to record spontaneous SPW-Rs in dorsal hippocampal slices from either mutants or wild type animals.

In the CA3 and CA1 of ventral hippocampal slices, however, clear differences between genotypes could be observed. In particular, in the CA3, SPW incidence (Fig. 4C, left-hand) was slightly but significantly increased in slices from *Hprt*$^{\alpha 3L185L\ +/0}$; *Pvalb*$^{Cre\ +/-}$ mice (1.64 ± 0.07 Hz; $P < 0.05$) compared with control mice (1.38 ± 0.09 Hz). In the CA1 (representative traces are shown in Supplementary Fig. 4), a general reduction of SPW incidence was observed compared with area CA3 regardless of the genotype (Fig. 4C, right-hand). This may be due to severed connectivity between areas CA3 and CA1 during slice preparation. In addition, the strength of the SPW-R generation in the CA3 and local CA3-independent generation of SPW-Rs in the CA1 are other factors that could modulate the incidence of CA1 SPW-Rs. Nevertheless, SPWs were more frequent (Fig. 4C, right-hand; Table 1) in CA1 of *Hprt*$^{\alpha 3L185L\ +/0}$; *Pvalb*$^{Cre+/-}$ mice compared with control mice (1.10 ± 0.09 Hz vs. 0.60 ± 0.06 Hz; $P < 0.001$). In the CA3, the area under the curve of SPWs (Fig. 4D, left-hand), which represents the sum of compound postsynaptic potentials, was not different between genotypes (Table 1; $P > 0.05$). There was no significant change in area under the curve of SPWs in the CA1 (Fig. 4D, right-hand; Table 1; $P > 0.05$). Interestingly, the number of ripples per SPW in the CA3 (Fig. 4E, left-hand) was significantly higher in *Hprt*$^{\alpha 3L185L\ +/0}$; *Pvalb*$^{Cre\ +/-}$ mice (3.37 ± 0.10, $P < 0.001$) compared with the control mice (2.76 ± 0.10) while, in the CA1, the number of ripples per SPW (Fig. 4E, right-hand) was comparable in *Hprt*$^{\alpha 3L185L+/0}$; *Pvalb*$^{Cre\ +/-}$ and control mice (Table 1, $P > 0.05$). Moreover, the CA3 ripple amplitude (Fig. 4F, left-hand) was smaller in slices of *Hprt*$^{\alpha 3L185L\ +/0}$; *Pvalb*$^{Cre\ +/-}$ mice (64 ± 5 μV; $P < 0.05$) compared with control mice (86 ± 6 μV). Interestingly, ripple amplitude in the CA1 (Fig. 4F, right-hand) was statistically unaltered (see Table 1 for details; $P > 0.05$). Lastly, analysis of ripple frequency in the CA3 (Fig. 4G, left-hand) revealed that *Hprt*$^{\alpha 3L185L\ +/0}$; *Pvalb*$^{Cre+/-}$ mice exhibited ripples with higher frequency (*Hprt*$^{\alpha 3L185L\ +/0}$; *Pvalb*$^{Cre\ +/-}$, 231 ± 2 Hz vs. *Hprt*$^{\alpha 3L185L\ +/0}$, 213 ± 3 Hz; $P < 0.001$). This parameter was unchanged in *Hprt*$^{\alpha 3L185L\ +/0}$; *Pvalb*$^{Cre\ +/-}$ mice (Fig. 4G, right-hand; see Table 1 for details; $P > 0.05$).

Collectively, the data obtained from recording in area CA3 and CA1 show that SPW-R properties are profoundly altered in slices of mice with hyperfunctionality of PV interneurons. Furthermore, an increased SPW incidence in the CA1 of *Hprt*$^{\alpha 3L185L\ +/0}$; *Pvalb*$^{Cre\ +/-}$ mice, suggests facilitated propagation of SPW-Rs in these animals.

Enhanced Neural Network Interaction During SPW-R Activity

To determine whether the propagation of SPW-Rs from area CA3 to area CA1 is facilitated in slices of *Hprt*$^{\alpha 3L185L\ +/0}$; *Pvalb*$^{Cre\ +/-}$ mice, extracellular field recordings were obtained simultaneously from both areas CA3 and CA1, and CA3-to-CA1 network interactions were analyzed (Fig. 5A–I). In line with the increase in SPW incidence in both areas CA3 and CA1 in *Hprt*$^{\alpha 3L185L\ +/0}$; *Pvalb*$^{Cre\ +/-}$ mice, the correlation of SPW activity (Fig. 5B,C) in CA3 and CA1 was significantly increased in these animals (0.62 ± 0.07) compared with control (0.28 ± 0.05; $P = < 0.001$). Increased correlation of SPW activity between CA3 and CA1 can result from augmented signal-to-noise ratio in area CA3 where the SPW-Rs are generated (Maier et al. 2003). Indeed, signal-to-noise ratio (Fig. 5D) in CA3 was almost doubled in *Hprt*$^{\alpha 3L185L\ +/0}$; *Pvalb*$^{Cre\ +/-}$ mice (93 ± 12) compared with controls (*Hprt*$^{\alpha 3L185L\ +/0}$, 46 ± 8; $P < 0.01$). Furthermore, there was a positive correlation between signal-to-noise ratio and CA3–CA1 correlation values (Fig. 5D,E; *Hprt*$^{\alpha 3L185L\ +/0}$; *Pvalb*$^{Cre\ +/-}$, $P < 0.01$, correlation coefficient = 0.70; *Hprt*$^{\alpha 3L185L\ +/0}$, $P < 0.05$, correlation coefficient = 0.53). Consistently, amplitude correlation of SPWs (Fig. 5F) was significantly increased in *Hprt*$^{\alpha 3L185L+/0}$; *Pvalb*$^{Cre\ +/-}$ mice (0.65 ± 0.07; $P < 0.01$) compared with control mice (0.34 ± 0.06), and SPW latency (Fig. 5G) from CA3 to CA1 was significantly shorter in *Hprt*$^{\alpha 3L185L\ +/0}$; *Pvalb*$^{Cre\ +/-}$ mice (6.1 ± 0.6 ms; $P < 0.05$) compared with control mice (11.6 ± 1.6 ms). We finally analyzed failures of SPW propagation (Fig. 5H,I) from CA3 to CA1 and observed fewer failures in *Hprt*$^{\alpha 3L185L\ +/0}$; *Pvalb*$^{Cre\ +/-}$ mice (0.35 ± 0.07) than in control mice (*Hprt*$^{\alpha 3L185L\ +/0}$, 0.54 ± 0.06; $P < 0.05$; Fig. 5H, I). Altogether, these data demonstrate an enhanced signal-to-noise ratio and a significantly more reliable propagation of SPW from area CA3 to area CA1 in slices of mice with hyperfunctionality of PV interneurons.

Correlation Between SPW-R Activity and Fear Memory Persistence

In order to test for possible correlation of individual network activity and fear memory persistence, we next examined SPW-R activity 1 hour after the second extinction session, that is, the time point when successful extinction was first observed in control groups, but not in *Hprt*$^{\alpha 3L185L\ +/0}$; *Pvalb*$^{Cre\ +/-}$ mice. Overall, *Hprt*$^{\alpha 3L185L\ +/0}$; *Pvalb*$^{Cre+/-}$ mice ($N = 8$ mice, $N = 37$ slices) in this experiment showed differences to control *Hprt*$^{\alpha 3L185L\ +/0}$ mice ($N = 8$ mice, $N = 40$ slices) that were similar to those observed in naïve mutants. Specifically, a higher incidence of SPW-Rs was evident in area CA1 (*Hprt*$^{\alpha 3L185L\ +/0}$; *Pvalb*$^{Cre\ +/-}$, 1.65 ± 0.07 Hz vs. *Hprt*$^{\alpha 3L185L\ +/0}$, 1.03 ± 0.09 Hz; $P < 0.05$), whereas in area CA3 no difference was evident (*Hprt*$^{\alpha 3L185L\ +/0}$; *Pvalb*$^{Cre\ +/-}$, 1.27 ± 0.05 Hz vs. *Hprt*$^{\alpha 3L185L\ +/0}$, 1.16 ± 0.05 Hz; $P > 0.05$). Interestingly, we observed differential effects of fear extinction training on other SPW-R properties in both genotypes (data shown in detail in Table 2).

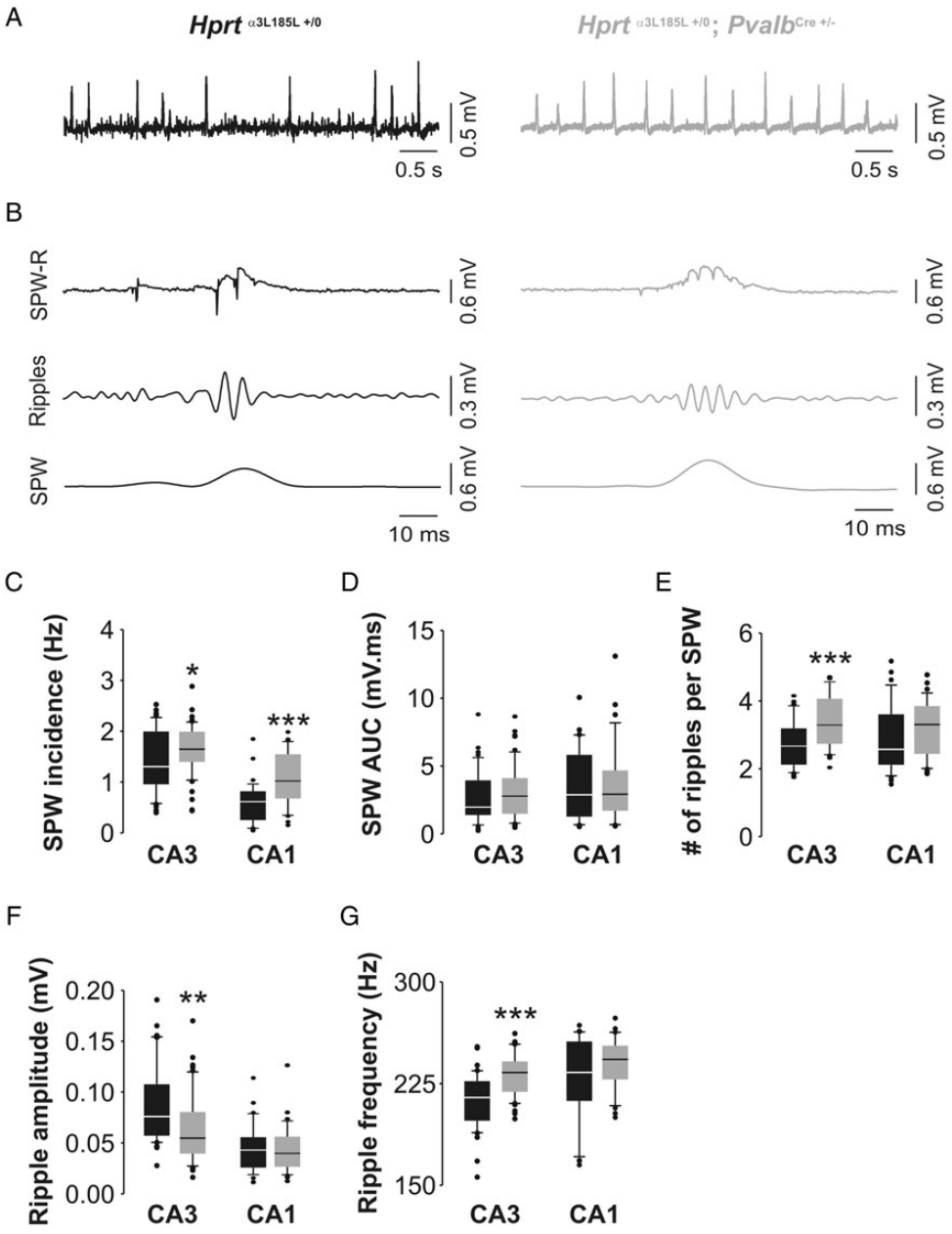

Figure 4. Incidence of SPW-R is increased in mice with enhanced functionality of PV interneurons ($Hprt^{\alpha 3L185L\ +/0}$; $Pvalb^{Cre\ +/-}$). (*A*) Example traces of SPW-Rs recorded in pyramidal cell layer of CA3 in horizontal hippocampal slice preparations. (*B*) Representative traces of SPW-R (top trace), ripples (middle trace), and SPW (bottom trace) of each genotype. (*C–G*) Summary graphs depicting differences in SPW-R properties in the CA3 and CA1 regions of $Hprt^{\alpha 3L185L\ +/0}$; $Pvalb^{Cre\ +/-}$ mice compared with control animals ($Hprt^{\alpha 3L185L\ +/0}$). Quantitative data on SPW occurrence (*C*), area under curve of SPWs (*D*), number of ripples per SPW (*E*), amplitude of ripple oscillations (*F*), and ripple frequency (*G*) are shown. The data in the graphs are shown as box plots. The median value is the horizontal line. The boundary of the box closest to zero indicates the 25th percentile and the boundary of the box farthest from zero indicates the 75th percentile. Whiskers (error bars) above and below the box indicate the 90th and 10th percentiles. Data points (single dots) beyond the 5th and 95th percentiles are also displayed. Student's *t*-test or Mann–Whitney *U* test was used to compare genotype effect in each region. Significant differences between genotypes are indicated with asterisks (*$P < 0.05$; **$P < 0.01$; ***$P < 0.001$).

Next, we analyzed freezing duration and parameters reflecting the strength of network interactions during SPW-Rs after the second extinction session E2 (Fig. 6A–E; Table 2). To minimize a potential effect of memory retrieval itself on hippocampal physiology we restricted testing of fear memory to a brief 2 min period in this session. Consistent with the results shown above (Fig. 1), $Hprt^{\alpha 3L185L\ +/0}$; $Pvalb^{Cre\ +/-}$ mice again showed increased freezing at the session E2 compared with control $Hprt^{\alpha 3L185L\ +/0}$ mice (Fig. 6B; $Hprt^{\alpha 3L185L\ +/0}$; $Pvalb^{Cre\ +/-}$, 74.1 ± 4.4% vs. $Hprt^{\alpha 3L185L\ +/0}$, 50.7 ± 4.2%; $P < 0.01$). Furthermore, CA3–CA1 event failure was significantly decreased in $Hprt^{\alpha 3L185L\ +/0}$; $Pvalb^{Cre\ +/-}$ mice compared with control mice (Fig. 6C; $Hprt^{\alpha 3L185L\ +/0}$; $Pvalb^{Cre\ +/-}$, 0.13 ± 0.02 vs. $Hprt^{\alpha 3L185L\ +/0}$, 0.46 ± 0.07; $P < 0.01$), increased CA3–CA1 correlation was observed (Fig. 6D; $Hprt^{\alpha 3L185L\ +/0}$; $Pvalb^{Cre\ +/-}$, 0.46 ± 0.04 vs. $Hprt^{\alpha 3L185L\ +/0}$, 0.27 ± 0.04; $P < 0.01$;), and the signal-to-noise ratio was increased in area CA3 (Fig. 6E; $Hprt^{\alpha 3L185L\ +/0}$; $Pvalb^{Cre\ +/-}$, 52 ± 5 vs. $Hprt^{\alpha 3L185L\ +/0}$, 25 ± 4; $P < 0.05$).

We next asked whether the observed changes in SPW-R activity would correlate with freezing behavior on an individual animal level, but did not find any correlation between freezing

Table 1 Properties of SPW-Rs in CA3 and CA1 of adult hippocampal slices

	SPW incidence (Hz)		SPW area under curve (mV. ms)		Number of ripples per SPW		Ripple amplitude (μV)		Ripple frequency (Hz)	
	CA3	CA1	CA3	CA1	CA3	CA1	CA3	CA1	CA3	CA1
	N = 13, 12, 5 n = 45, 53, 29	N = 13, 11, 5 n = 37, 35, 20	N = 13, 12, 5 n = 45, 53, 29	N = 13, 11, 5 n = 37, 35, 20	N = 13, 12, 5 n = 41, 53, 28	N = 13, 11, 5 n = 36, 35, 20	N = 13, 12, 5 n = 41, 53, 28	N = 13, 11, 5 n = 36, 35, 20	N = 13, 12, 5 n = 41, 53, 28	N = 13, 11, 5 n = 36, 35, 20
$Hprt^{\alpha 3L185L+/0}$	1.38 ± 0.09	0.60 ± 0.06	2.68 ± 0.56	3.58 ± 0.42	2.76 ± 0.10	2.88 ± 0.16	86 ± 6	45 ± 4	213 ± 3	230 ± 5
$Hprt^{\alpha 3L185L+/0}$; $Pvalb^{Cre+/-}$	1.64 ± 0.07*	1.10 ± 0.09***	3.03 ± 0.27	3.60 ± 0.48	3.37 ± 0.10***	3.20 ± 0.14	64 ± 5[a]	45 ± 4	231 ± 2***	239 ± 3

Number of animals (*N*) and number of slices (*n*) are indicated for each genotype: first value: $Hprt^{\alpha 3L185L+/0}$ (control), second value: $Hprt^{\alpha 3L185L+/0}$; $Pvalb^{Cre+/-}$; third value: $Hprt^{\alpha 3L185L+/0}$; $Camk2a^{Cre+/-}$. The data are presented as mean ±SEM.
*Indicates significant difference to control mice. Student's *t*-test or Mann–Whitney *U* test was used to compare genotype effect.

behavior and SPW-R properties within a group ($n = 8$ animals each, data not shown). However, after pooling data from both genotypes, a significant negative correlation was observed between CA3–CA1 propagation failure (i.e., increased network interactions during SPW-Rs) and freezing duration (Supplementary Fig. 5A, Pearson's R = –0.536; $P < 0.05$). Furthermore, a significant positive correlation between SPW incidence in area CA1 and freezing duration became evident (Supplementary Fig. 5B, R = 0.538; $P < 0.05$), but freezing duration and CA3–CA1 SPW correlation, CA3 signal-to-noise ratio, or CA3–CA1 latency did not correlate (R = 0.485, R = 0.194, or R = –0.130, respectively; $P > 0.05$, each).

Correlation Between Parvalbumin Expression and Fear Memory Persistence

Recently, specific levels of parvalbumin immunoreactivity (classified as low, intermediate low, intermediate high, and high) in the dorsal hippocampal CA3b region were established as cellular anatomical correlate of PV network configuration and its involvement in memory consolidation in a novel-object recognition learning task (Donato et al. 2013). We examined this parameter in ventral and dorsal hippocampi of mice 1 h after the second extinction session E2 (Fig. 7A). To minimize the effect of memory retrieval itself on PV gene expression we again restricted the session to 2 min. Again, $Hprt^{\alpha 3L185L+/0}$; $Pvalb^{Cre+/-}$ mice showed increased freezing at the session E2 compared with control $Hprt^{\alpha 3L185L+/0}$ mice (Fig. 7B; $Hprt^{\alpha 3L185L+/0}$; $Pvalb^{Cre+/-}$, 65.5 ± 7.6% vs. $Hprt^{\alpha 3L185L+/0}$, 37.3 ± 8.2%; $P < 0.05$), confirming our initial findings. PV signals were significantly increased in the ventral hippocampus of $Hprt^{\alpha 3L185L+/0}$; $Pvalb^{Cre+/-}$ mice compared with control animals, whereas no difference was observed in the dorsal hippocampus of the 2 animal groups (Fig. 7C,D; $P < 0.001$ and $P > 0.05$, respectively). We then asked whether freezing duration at E2 would correlate with the proportion of ventral hippocampal interneurons in the 4 groups classified "low", "intermediate low", "intermediate high," and "high". Again there was no correlation of data within a group, but when data from both genotypes were pooled ($n = 15$ animals), the fraction of interneurons classified "intermediate high" positively and significantly correlated with freezing times (Supplementary Fig. 6A; Pearson's R = 0.59, $P < 0.05$), while the fraction of interneurons classified "low" decreased freezing time-dependently and negatively and significantly correlated with freezing times (Supplementary Fig. 6A; Pearson's R = –0.74, $P < 0.01$). Pearson's R for "high" and "intermediate low" neurons did not indicate significant correlation (R = 0.49 and R = –0.34, respectively, $P > 0.05$). Also, in the dorsal hippocampus, no correlation was observed between freezing times and fractions of PV interneurons in the 4 different groups (Supplementary Fig. 6B).

Discussion

Genetic and experience-dependent alterations in perisomatic inhibition may provide a disposition to altered fear memory and anxiety states. We used here an animal model with PV interneuron-targeted expression of the gain-of-function GlyR RNA variant $\alpha 3L^{185L}$ (Winkelmann et al. 2014) to study this relation. GlyR $\alpha 3L^{185L}$ expression is increased in hippocampectomies of patients with temporal lobe epilepsy (Eichler et al. 2008; Legendre et al. 2009). In our animal model, the presynaptic expression of GlyR $\alpha 3L^{185L}$ results in enhancement of the functional impact of PV interneurons within the neural network (Winkelmann et al. 2014). Our data identify a pronounced effect of such genetic

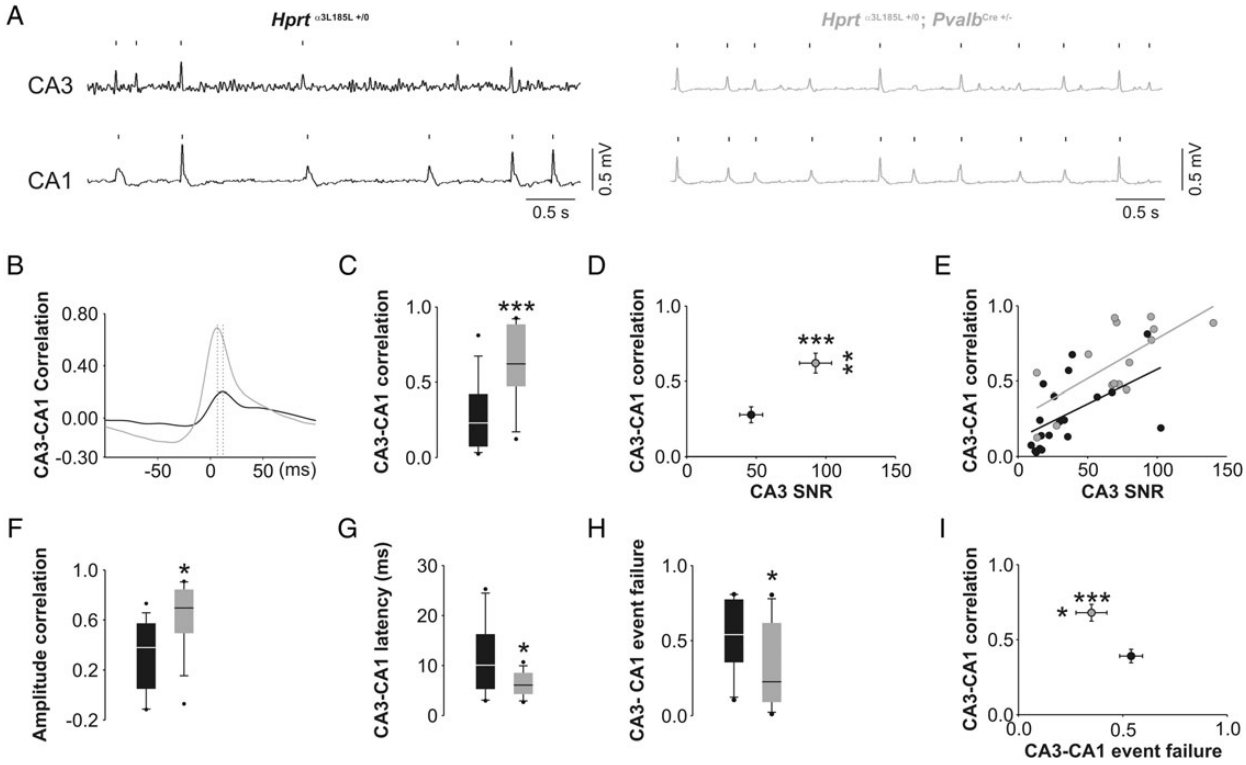

Figure 5. CA3–CA1 network interaction during SPW-R activity is facilitated in mice with enhanced functionality of PV interneurons ($Hprt^{\alpha 3L185L\ +/0}$; $Pvalb^{Cre\ +/-}$). (*A*) Example traces of low-pass filtered (3–45 Hz) SPW-Rs recorded simultaneously in pyramidal cell layer of areas CA3 (top) and CA1 (bottom) in horizontal hippocampal slice preparations. (*B*) The representative example of cross-correlation of SPWs indicates increased correlation and decreased latency in $Hprt^{\alpha 3L185L\ +/0}$; $Pvalb^{Cre\ +/-}$ mice. The dashed lines indicate peak and latency. (*C*) Summary graph indicating a significant increase in CA3–CA1 correlation of SPWs in $Hprt^{\alpha 3L185L\ +/0}$; $Pvalb^{Cre\ +/-}$ mice ($n = 15$ slices, $N = 4$ mice) compared with $Hprt^{\alpha 3L185L\ +/0}$ control mice ($n = 19$ slices, $N = 5$ mice). (*D*) Mean values of CA3–CA1 correlation of SPWs (*y* axis) plotted against mean values of signal-to-noise ratio (SNR, *x* axis) for both genotypes. Note that $Hprt^{\alpha 3L185L\ +/0}$; $Pvalb^{Cre\ +/-}$ mice exhibited a significant increase of SNR in CA3 as well as CA3–CA1 correlation of SPWs. (*E*) Individual values of CA3–CA1 correlation (*y* axis) and SNR (*x* axis) were plotted against each other. Note that a high CA3–CA1 correlation correlates with an increased signal-to-noise ratio in CA3 of the hippocampal slices. (*F*) CA3–CA1 amplitude correlation of SPWs were increased in $Hprt^{\alpha 3L185L\ +/0}$; $Pvalb^{Cre+/-}$ mice. (*G*) CA3–CA1 SPW latency was decreased in $Hprt^{\alpha 3L185L\ +/0}$; $Pvalb^{Cre\ +/-}$ mice. (*H*) The ratio of failures of SPW propagation from CA3 to CA1 was decreased in $Hprt^{\alpha 3L185L\ +/0}$; $Pvalb^{Cre\ +/-}$ mice. (*I*) Mean values of CA3–CA1 correlation of SPWs (*y* axis) were plotted against the mean values of CA3–CA1 event failures (*x* axis) for each genotype. Note that slices with increased correlation tended to have decreased propagation failures. The data in the graphs (*C*, *F*, *G*, and *H*) are shown as box plots. The horizontal line in the middle is the median value. The boundary of the box closest to zero indicates the 25th percentile and the boundary of the box farthest from zero indicates the 75th percentile. Whiskers (error bars) above and below the box indicate the 90th and 10th percentiles. Data points (single dots) beyond the 5th and 95th percentiles are also displayed. Student's *t*-test or Mann–Whitney *U* test was used to compare genotype effect. Pearson Product Moment Correlation was used to assess the correlation between 2 parameters. Significant differences between $Hprt^{\alpha 3L185L\ +/0}$; $Pvalb^{Cre\ +/-}$ and $Hprt^{\alpha 3L185L\ +/0}$ control mice are indicated with asterisks (*$P < 0.05$, **$P < 0.01$, ***$P < 0.001$).

Table 2 Properties of SPW-Rs in CA3 and CA1 of adult hippocampal slices in fear-exposed mice investigated at the second day of extinction training (E2)

	SPW incidence (Hz)		SPW area under curve (mV ms)		Number of ripples per SPW		Ripple amplitude (μV)		Ripple Frequency (Hz)	
	CA3 $N = 8, 8$ $n = 39, 37$	CA1 $N = 8, 8$ $n = 37, 35$	CA3 $N = 8, 8$ $n = 40, 37$	CA1 $N = 8, 8$ $n = 37, 35$	CA3 $N = 8, 8$ $n = 40, 37$	CA1 $N = 8, 8$ $n = 36, 35$	CA3 $N = 8, 8$ $n = 39, 37$	CA1 $N = 8, 8$ $n = 40, 36$	CA3 $N = 8, 8$ $n = 40, 37$	CA1 $N = 8, 8$ $n = 35, 33$
$Hprt^{\alpha 3L185L+/0}$	1.16 ± 0.05	1.03 ± 0.09#	1.09 ± 0.15#	1.13 ± 0.17#	2.45 ± 0.11	2.38 ± 0.11	63 ± 7#	39 ± 3	215 ± 2	229 ± 3
$Hprt^{\alpha 3L185L+/0}$; $Pvalb^{Cre+/-}$	1.27 ± 0.05#	1.65 ± 0.07*,#	1.62 ± 0.17#	1.88 ± 0.17*	2.78 ± 0.09#	2.89 ± 0.12*	63 ± 5	44 ± 3	216 ± 1#	231 ± 2

Number of animals (*N*) and number of slices (*n*) are indicated for each genotype. The data are presented as mean ± SEM.
*Indicates significant ($P < 0.05$) difference between genotypes.
#Indicates significant fear training effect ($P < 0.05$) in comparison to naïve animals (Table 1).

enhancement of perisomatic-targeting inhibitory interneurons on the generation and propagation of hippocampal SPW-Rs and to the persistence of contextual fear memory. We propose that the increased SPW-R activity in these mice may represent a physiological correlate of reconsolidation of the original fear memory, outcompeting fear extinction.

In our previous study, $Hprt^{\alpha 3L185L\ +/0}$; $Pvalb^{Cre\ +/-}$ mice presented with increased anxiety but normal spatial memory (Winkelmann et al. 2014). The ventral hippocampus, which is enriched in PV interneurons as compared with the dorsal hippocampus (Caballero et al. 2013), is known to control emotional aspects of behavior and memory formation (Bannerman et al.

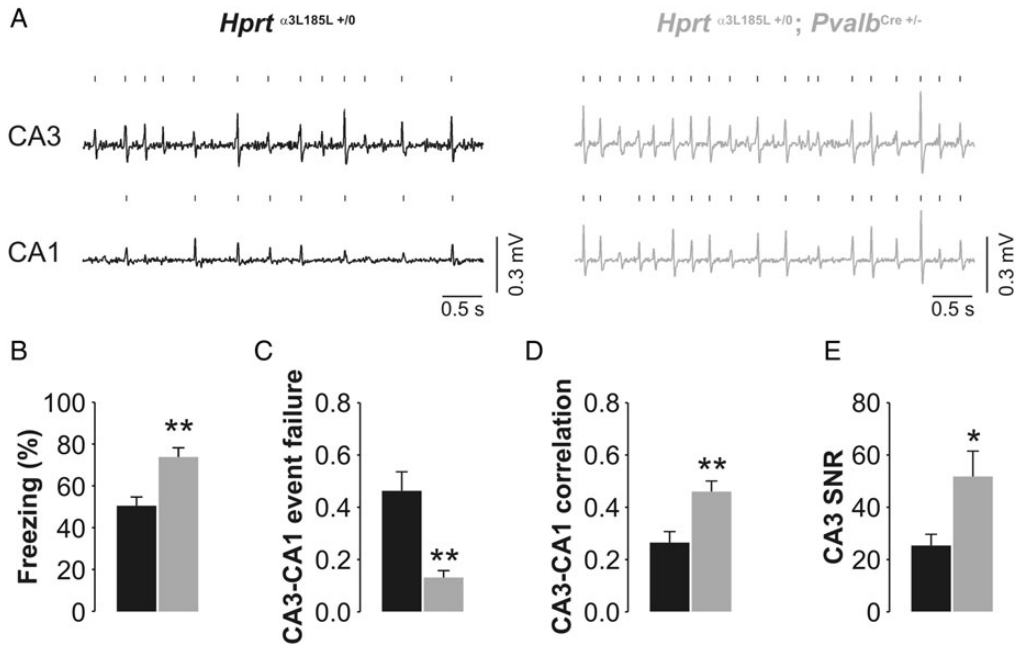

Figure 6. The strength of CA3–CA1 network interaction during SPW-R activity is correlated with fear behavior at the second extinction session, E2. (*A*) Example traces of low-pass filtered (3–45 Hz) SPW-Rs recorded simultaneously in pyramidal cell layer of areas CA3 (top) and CA1 (bottom) from control mice ($Hprt^{\alpha 3L185L\ +/0}$) and $Hprt^{\alpha 3L185L\ +/0}$; $Pvalb^{Cre\ +/-}$ mice. Note the increased SPW propagation in mice with enhanced functionality of PV interneurons. (*B*) Freezing duration (percent time of 2 min) at E2 was increased in $Hprt^{\alpha 3L185L\ +/0}$; $Pvalb^{Cre\ +/-}$ compared with the control mice ($Hprt^{\alpha 3L185L\ +/0}$) (*C*) Similar to naïve mice, CA3-CA1 propagation failures of SPWs were decreased in mice with enhanced functionality of PV interneurons ($Hprt^{\alpha 3L185L\ +/0}$; $Pvalb^{Cre\ +/-}$). (*D*) CA3–CA1 correlation of SPWs, and (*E*) signal-to-noise ratio (SNR) in area CA3 were increased in $Hprt^{\alpha 3L185L\ +/0}$; $Pvalb^{Cre\ +/-}$ mice. Significant differences between $Hprt^{\alpha 3L185L\ +/0}$; $Pvalb^{Cre\ +/-}$ and $Hprt^{\alpha 3L185L\ +/0}$ control mice are indicated with asterisks (*$P < 0.05$, **$P < 0.01$).

2004, 2014). Therefore, we asked whether PV interneuron-dependent function in the ventral hippocampus, which is responsible for the formation and stability of contextual fear memories, may be altered in $Hprt^{\alpha 3L185L\ +/0}$; $Pvalb^{Cre\ +/-}$ mice. Indeed, our data show that these animals are clearly impaired in contextual fear extinction and maintain elevated levels of freezing behavior throughout their exposure to a 5-day extinction training period. The deficit was reproduced in subsequent electrophysiological and immunohistochemical experiments. Control animals, in contrast, showed efficient extinction of fear memory and reduced freezing already after a single extinction training session. Unaltered freezing of the mutant mice during the pretraining period and normal pain responsiveness exclude a priori motor or sensory deficits that could affect the performance in contextual fear-driven memory tasks. Thus, we conclude that hyperfunctionality of PV interneurons in $Hprt^{\alpha 3L185L\ +/0}$; $Pvalb^{Cre\ +/-}$ mice contributes to impairment of extinction of contextual fear memory.

The ventral hippocampus plays a key role in fear extinction, but other brain regions such as amygdala and prefrontal cortex (PFC) are also critically involved (Milad and Quirk 2002; Bissonette et al. 2014; Courtin et al. 2014; Sparta et al. 2014). The observed behavioral phenotype thus could be related to altered weight and function of PV interneurons in the local network of different fear memory-related regions in the brain. In fact, a recent paper (Brown et al. 2015) described a disturbance of auditory cued fear memory extinction after transgenic knock down of Gad1 gene-encoded 67-kDa protein isoform of glutamic acid decarboxylase (GAD67) in PV interneurons associated with reduction in frequency of spontaneous inhibitory events in the PFC. However, we found no evidence for an alteration in this amygdala- and frontal cortex-dependent task. While this does not rule out a contribution of altered PV neuron activity in these regions during contextual fear extinction, it demonstrates the principle ability of $Hprt^{\alpha 3L185L\ +/0}$; $Pvalb^{Cre\ +/-}$ mice to extinguish fear memories similarly to control animals and suggests that the altered memory-related network activity in the ventral hippocampus of these mice may play an important role in their context fear extinction deficit. Several reasons might account for the discrepancy between the Gad1 animal model and our mouse model. Most importantly, loss of function and gain of function in perisomatic-targeting PV interneurons may not affect all brain areas equally well, depending on the weight and function of these neurons in the local network. Moreover, activation of PV interneuron networks via GlyR $\alpha 3L^{185L}$ may be affected by glycine and/or zinc (a well-known modulator of GlyRs (Laube et al. 2000; McCracken et al. 2013)) in the hippocampus, for example, at mossy fiber terminals in area CA3 (Lee et al. 2009; Kubota et al. 2010; Winkelmann et al. 2014). It would indeed be interesting to clarify whether Gad1 knock down in PV interneurons also affects the generation and propagation of hippocampal SPW-Rs.

PV-neurons targeting perisomatic region of the principal glutamatergic neurons in the ventral hippocampus regulate their output, that is the synchrony of action potentials generated by principal cell population (Miles et al. 1996; Csicsvari et al. 2000). This is specifically important during memory-relevant network oscillation patterns such as SPW-Rs determining the ability to form specific memory “ensembles” (Wilson and McNaughton 1994; Stark et al. 2014). We therefore specifically investigated the SPW-Rs in the ventral hippocampal slice preparations, known to be generated in a PV-neuron dependent manner (Hajos et al. 2013; Schlingloff et al. 2014). The observed alterations of SPW-R appear to be intrinsic to the ventral hippocampus and occur independently of its afferent connectivity. Our data suggest

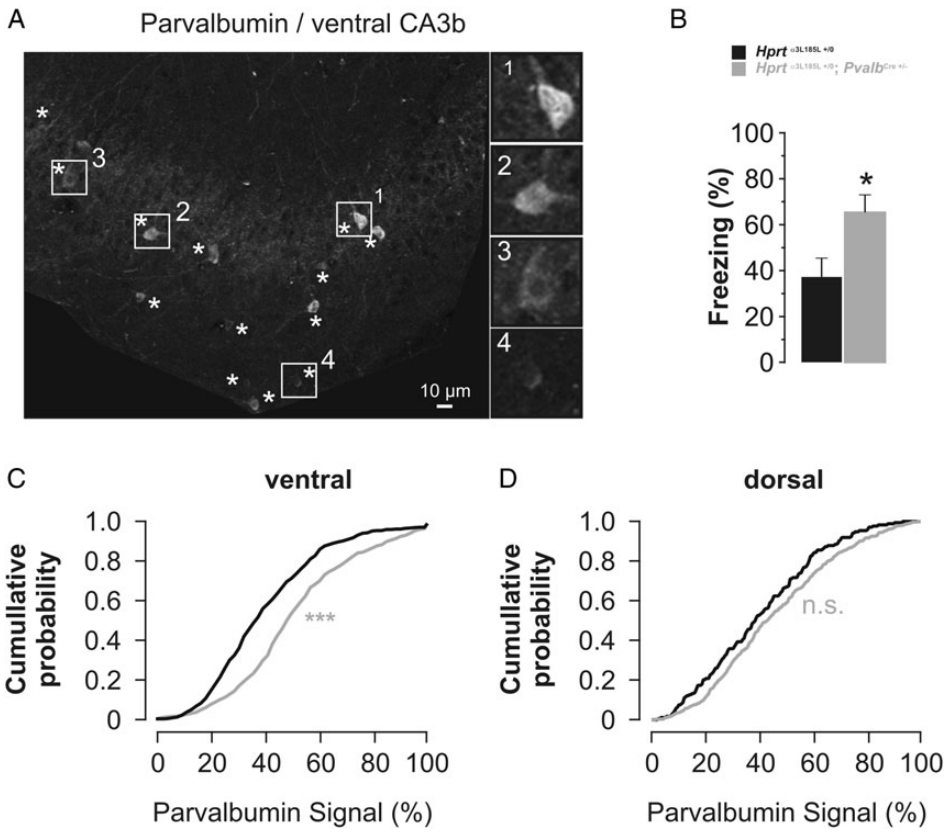

Figure 7. Correlation of parvalbumin signals in the CA3b region of the ventral hippocampus with fear behavior at the second extinction session, E2. (*A*) Representative image shows maximum intensity projections of *z*-stacks with parvalbumin signals in CA3b regions of the ventral hippocampus. Scale bars: 10 µm. Identified PV interneurons are indicated by asterisks. Numbering 1 to 4 of boxed regions and the insets right-hand at higher magnification show representative PV neurons classified as (from top to bottom) "high", "intermediate high", "intermediate low", and "low". (*B*) Freezing duration (percent time of 2 min) at E2 of mice processed for parvalbumin immunohistochemistry was significantly different between control (black bar) and $Hprt^{\alpha 3L185L\ +/0}$; $Pvalb^{Cre\ +/-}$ mice (gray bar). (*C*,*D*) Cumulative plots of the relative parvalbumin signal intensities from control animals and $Hprt^{\alpha 3L185L\ +/0}$; $Pvalb^{Cre\ +/-}$ mice reveal significant ($P < 0.001$) differences in the ventral (*C*), not dorsal (*D*), hippocampus. Statistical analysis was performed using Kolmogorov–Smirnov test.

that an increased perisomatic inhibition in the hippocampus of $Hprt^{\alpha 3L185L\ +/0}$; $Pvalb^{Cre\ +/-}$ mice could enhance the reactivation of previously formed fear memory ensembles and result in exaggerated fear behavior resistant to extinction.

In addition to changes in network activity, decreased baseline transmission in the Schaffer Collateral-CA1 pathway (Winkelmann et al. 2014) might also contribute to the observed behavior. However, a recent paper has demonstrated that acute pharmacogenetic inhibition of principal glutamatergic neurons in the ventral hippocampus within a 6 h time window after fear training (consolidation phase) results in impaired consolidation of contextual fear memory (Zhu et al. 2014), which was not observed with our protocol.

To date, the role of PV neuron activity in the ventral hippocampus in relation to persistence of fear memories has not been investigated. We could show that SPW-R activity is similarly enhanced in both behaviorally naïve and trained $Hprt^{\alpha 3L185L\ +/0}$; $Pvalb^{Cre\ +/-}$ mice, indicating that the gene mutation but not the training determines the degree of SPW-R activity in our model. Thus it can be expected that increased SPW-R activity will also be evident in vivo in $Hprt^{\alpha 3L185L\ +/0}$; $Pvalb^{Cre\ +/-}$ mice (Lu et al. 2011; Maier et al. 2012), in both the conditioned and unconditioned situations. The role of SPW-R in memory consolidation is firmly established and indeed, the propensity for SPW-R activity correlated with the level of fear memory during extinction in our experiments. *In vivo*, to correlate SPW-R activity with memory strength, behavioral state (e.g., sleep; Wilson and McNaughton 1994; Kudrimoti et al. 1999; Stark et al. 2014) of recording needs to be taken into consideration. Nevertheless, such recordings would likely not be sufficient to discriminate SPW-R functions in the re-consolidation of the original trace versus consolidation of extinction memory, which is the critical question arising from the current study. Rather, systematic interference (e.g., pharmacogenetics, optogenetics) in vivo will be necessary to address these points in future studies.

In a previous study (Winkelmann et al. 2014), $Hprt^{\alpha 3L185L\ +/0}$; $Pvalb^{Cre\ +/-}$ mice presented with an anxiety phenotype and mild freezing behavior measured in an open field. However, post-training and retrieval values in the contextual and the auditory cued paradigms confirmed that the levels of conditioned fear were similar between genotypes before extinction started. We further found no evidence for pretraining increase of anxiety in the mutants, indicating an aversiveness of the training context per se. Therefore, we suggest that the observed behavioral phenotype is related to a specific enhancement of the stability of contextual fear memory in $Hprt^{\alpha 3L185L\ +/0}$; $Pvalb^{Cre\ +/-}$ mice.

Current concepts suggest that memory traces become reactivated during fear memory retrieval and that fear memory is reconsolidated in an updated form upon the reactivation. Therein, the extinction of fear memories, that is, the reduction of fear responding upon repetitive nonreinforced retrieval, competes with reconsolidation of the original trace, a process of renewed

storage without decay in performance (Eisenberg et al. 2003; de la Fuente et al. 2011). Reconsolidation is typically seen after one or few retrieval sessions and utilizes similar cellular and molecular processes as the original consolidation (Nader et al. 2000; Debiec et al. 2002). Strikingly, reconsolidation of contextual fear is accompanied by increased activation of amygdala and hippocampus, whereas extinction results in activation of mPFC and amygdala (Mamiya et al. 2009).

The deficit of *Hprt*$^{\alpha 3L185L\ +/0}$; *Pvalb*$^{Cre\ +/-}$ mice to extinguish context fear memories thus allowed us to investigate potential physiological correlates of fear memory persistence in the hippocampus. SPW-Rs, which are generated via parvalbuminergic local networks in the hippocampus, are prime candidates in this respect. In vivo, SPW-Rs occur during slow-wave sleep and likely represent stored information that is replayed in the hippocampus and finally transferred to the neocortex, for example, during memory consolidation (Buzsaki 1989; Buzsaki et al. 1992; Wilson and McNaughton 1994; Nadasdy et al. 1999). Increased density and magnitude of hippocampal SPW-Rs have already been described following memory retrieval (Eschenko et al. 2008). Therefore, it is plausible to assume that the enhanced SPW-R activity and SPW propagation observed in *Hprt*$^{\alpha 3L185L\ +/0}$; *Pvalb*$^{Cre\ +/-}$ mice may be related to an altered (re-)consolidation of fear memory. Indeed, the mutant mice recovered a profound initial freezing response after each extinction training and most profound genotype difference were observed during the extinction session E2, the first to present both extinction and reconsolidation effects. This indicates a failure of overnight consolidation of fear extinction and reconsolidation-like persistence of the original fear memory trace. It is important to discriminate this from the spontaneous recovery of successfully extinguished fear memory after the passage of time (Myers and Davis 2007). Whether or not this latter phenomenon may be affected by PV network activity unfortunately cannot be assessed in our model due to the a priori deficit in extinction memory.

If altered activity of PV neurons in ventral hippocampus is a physiological correlate of the observed extinction deficits, relevant PV-dependent network activities in this structure should display corresponding changes. Indeed basic properties of SPW-Rs (Maier et al. 2003, 2009; Kanak et al. 2013; Kranig et al. 2013) were changed in both slices from naïve *Hprt*$^{\alpha 3L185L\ +/0}$; *Pvalb*$^{Cre\ +/-}$ mice and in slices taken during fear memory extinction. We observed a similar increase in the incidence of SPW-Rs in area CA1 and in the network interaction between CA3 and CA1 subfields with and without behavioral manipulation, suggesting that these effects are primarily driven by the genetic manipulation. Moreover, some basic properties of SPW-Rs like SPW size, number of ripples, ripple amplitude and ripple frequency in area CA3 and CA1 seem to be affected by the behavioral training.

We chose the enhanced CA3–CA1 network interactions during SPW-Rs as the most robust genetically induced effect of *Hprt*$^{\alpha 3L185L\ +/0}$; *Pvalb*$^{Cre\ +/-}$ mutation to further study the potential association of enhanced SPW-R activity with fear memory stability. In these experiments, slices were analyzed during a 6-h post-learning rest period that is thought to be most critical for SPW-R mediated consolidation mechanisms (Buzsaki 1989; Wilson and McNaughton 1994; Chrobak and Buzsaki 1996; Kudrimoti et al. 1999; Marshall et al. 2006). Although we did not find clear correlation between freezing behavior and SPW-R properties within genotypes, correlation analysis of the pooled data suggests that increased SPW-R activity might relate to reconsolidation of the initially encoded fear memory during extinction training, at the expense of consolidating the newly formed memory for fear extinction. Furthermore, similar strength and significance of correlation between SPW-Rs and freezing between groups support the concept of encoding memory strength in a quantitative manner in the hippocampus (Kirwan et al. 2008; Shrager et al. 2008).

As augmented SPW-R in *Hprt*$^{\alpha 3L185L\ +/0}$; *Pvalb*$^{Cre\ +/-}$ mice were observed both in naïve animals and following extinction learning, it can be assumed that increased propagation of information has occurred during both the memory consolidation and the extinction/reconsolidation process. In fact, although contextual conditioning tends to produce lower freezing values than cued conditioning it is hard to extinguish, particularly in mice. For instance, in a study by Golub et al. (2009) contextual fear conditioning with a highly aversive unconditional stimulus and 75% freezing allowed for only 25% extinction, even though the extinction training was 3 times as long as in the our experiments (Golub et al. 2009). Thus, even though freezing levels after memory acquisition in our experiments did not significantly differ between genotypes, it should be considered that the dynamics of fear memory acquisition and fear memory modification in *Hprt*$^{\alpha 3L185L\ +/0;\ Pvalb Cre\ +/-}$ mice might be more generally altered, depending on the training conditions. It is plausible to assume that in our experiments SPW-R activity may have led to a more stable fear memory trace during the initial training or as a consequence of state-specific network activity patterns during memory retrieval.

During context fear learning mossy fibers form filopodia onto PV interneurons in area CA3 of the dorsal hippocampus (Ruediger et al. 2011). Moreover, contextual fear conditioning and pharmacogenetic activation of PV interneurons induce a high activity state that is reflected in PV immunoreactivity in dorsal area CA3b and correlation with performance in the novel object recognition task (Donato et al. 2013). Thus, we hypothesized that genetic enhancement of PV network configuration in our mutants might induce changes in PV expression related to fear memory. Indeed our investigation of this immunohistochemical parameter revealed a generally increased PV signal intensity in ventral CA3b of mutants compared with control animals. Although we did not find correlation between freezing behavior and PV signal intensity within genotypes, the proportion of low and intermediate high states of PV interneurons in ventral CA3b of pooled data from both genotypes were negatively and positively, respectively, correlated with freezing duration during extinction at E2. In contrast, we did not find any correlation between proportion of interneurons with different parvalbumin signal intensities in the dorsal hippocampus and freezing duration during extinction at E2. Accordingly, we have previously demonstrated unaltered performance of *Hprt*$^{\alpha 3L185L\ +/0}$; *Pvalb*$^{Cre\ +/-}$ mice in a novel-object recognition task and a reward-based 8-arm radial maze test (Winkelmann et al. 2014).

Our results are in good agreement with a division of labor between dorsal and ventral hippocampal regions with regard to contextual memory processing of spatial and contextual emotional aversive stimuli, respectively. This is also in line with the differential impact of stress on hippocampal physiology along the dorso-ventral axis (Maggio and Segal 2007, 2009) and with anatomical evidence that suggests PFC and the hippocampus have segregated functional reciprocal connections to each other (Prasad and Chudasama 2013): the “dorsal pathway” connecting the dorsal PFC (retrosplenial, anterior cingulate, and orbital cortex etc.) and dorsal hippocampus involved in acquisition and relearning of fear memory, while the ventral pathway connecting the ventral PFC (prelimbic, infralimbic cortex etc.) and ventral hippocampus takes role in extinction-related processes (Prasad and Chudasama 2013; Hamilton and Brigman 2015; Rozeske et al. 2015). Homeostatic plasticity of PV interneurons in different hippocampal subdivisions and their impact on generation and

propagation of SPW-Rs may provide important cellular and network correlates of these mnemonic functions.

Extinction deficits and anxiety often co-occur (Zeitlin et al. 2012; Olsen et al. 2014; Pinna and Rasmusson 2014). In particular, resistance to fear extinction is a hallmark of posttraumatic stress disorder (PTSD) and is observed in rodent models of this disease (VanElzakker et al. 2014); targeting extinction therefore has been suggested as effective therapeutic approach to this disorder (Parsons and Ressler 2013). However, the induction of a full PTSD-like phenotype in $Hprt^{\alpha 3L185L\ +/0}$; $Pvalb^{Cre\ +/-}$ mice by fear conditioning is rather unlikely, since we did not observe neutral context generalization or extinction-resistance to a conditioned tone. Nevertheless, our study clearly identified a susceptible hippocampal state associated with contextual fear memory persistence in $Hprt^{\alpha 3L185L\ +/0}$; $Pvalb^{Cre\ +/-}$ mice. This discovery can also be relevant for the treatment of neuropsychiatric comorbidities of patients with mTLE, which present with interictal anxiety (Currie et al. 1971; Beyenburg et al. 2005). Indeed, fear and anxiety are some of the most frequent and clinically important comorbid disorders in mTLE patients (Vazquez and Devinsky 2003; Beyenburg et al. 2005). We observed increased expression of the GlyR $\alpha 3L^{185L}$ RNA variant in lobectomies of the mesial temporal lobe (Eichler et al. 2008, 2009), a hippocampal region corresponding to the ventral hippocampus in our animal model of epilepsy studied here. Interestingly, impaired extinction of fear was already reported in a mouse model of TLE (Lesting et al. 2011). This supports our previous postulate that spatiotemporal dynamics of GlyR RNA editing in PV interneurons of mTLE hippocampi and resulting impairment of contextual fear memory extinction contribute to neuropsychiatric comorbidities of the disease (Winkelmann et al. 2014). Furthermore, our results can be useful as a diagnostic tool in mTLE (Bragin et al. 2002; Axmacher et al. 2008).

Supplementary material

Supplementary Material can be found at http://www.cercor.oxfordjournals.org/ online.

Funding

This work was supported by the Bundesministerium für Bildung und Forschung BMBF (Era-Net NEURON II CIPRESS to J.C.M.) and the Helmholtz Association (VH-NG-246 to J.C.M.). Furthermore, funding by the excellence cluster NeuroCure, the Deutsche Forschungsgemeinschaft DFG (graduate college GRK 1123 "Cellular mechanisms of learning and memory consolidation", SFB-TR3 TPB5 to J.C.M., SFB779 TPB5 to O.S., Priority Programme SPP 1784 ME2075/7-1 to J.C.M., He1128/16-1 to UH), German Israeli Project Cooperation and the German Research Foundation (DIP) project to U.H. and O.S., and the Hertie Foundation are acknowledged. IM is a scholar of the Leibniz Graduate School "Synaptogenetics". Funding to pay the Open Access publication charges for this article was provided by the Technical University Braunschweig, Germany.

Notes

We thank Günther Schütz (German Cancer Research Center, Heidelberg, Germany) for kindly providing us with the Camk2a-iCre BAC (CKC) mouse line. We thank Anne Schäfer, Andra Eisenmann, and Carola Bernert for excellent technical assistance, and Sebastian Tausch as well as Maren Wendt for managing our transgenic mouse colonies and for genotyping the animals. We are also grateful for technical help to Dr H.-J. Gabriel (Charité Universitätsmedizin Berlin, Germany). Finally, we thank Maysalun Sader (Otto-von-Guericke-University Magdeburg, Germany) for helping with the behavioral experiments. *Conflict of Interest*: None declared.

References

Albrecht A, Bergado-Acosta JR, Pape HC, Stork O. 2010. Role of the neural cell adhesion molecule (NCAM) in amygdalo-hippocampal interactions and salience determination of contextual fear memory. Int J Neuropsychopharmacol. 13:661–674.

Albrecht A, Caliskan G, Oitzl MS, Heinemann U, Stork O. 2013. Long-lasting increase of corticosterone after fear memory reactivation: anxiolytic effects and network activity modulation in the ventral hippocampus. Neuropsychopharmacology. 38:386–394.

Axmacher N, Helmstaedter C, Elger CE, Fell J. 2008. Enhancement of neocortical-medial temporal EEG correlations during non-REM sleep. Neural Plast. 2008:563028.

Bannerman DM, Rawlins JN, McHugh SB, Deacon RM, Yee BK, Bast T, Zhang WN, Pothuizen HH, Feldon J. 2004. Regional dissociations within the hippocampus–memory and anxiety. Neurosci Biobehav Rev. 28:273–283.

Bannerman DM, Sprengel R, Sanderson DJ, McHugh SB, Rawlins JN, Monyer H, Seeburg PH. 2014. Hippocampal synaptic plasticity, spatial memory and anxiety. Nat Rev Neurosci. 15:181–192.

Battaglia FP, Benchenane K, Sirota A, Pennartz CM, Wiener SI. 2011. The hippocampus: hub of brain network communication for memory. Trends Cogn Sci. 15:310–318.

Beyenburg S, Mitchell AJ, Schmidt D, Elger CE, Reuber M. 2005. Anxiety in patients with epilepsy: systematic review and suggestions for clinical management. Epilepsy Behav. 7:161–171.

Bissonette GB, Bae MH, Suresh T, Jaffe DE, Powell EM. 2014. Prefrontal cognitive deficits in mice with altered cerebral cortical GABAergic interneurons. Behav Brain Res. 259:143–151.

Bragin A, Wilson CL, Staba RJ, Reddick M, Fried I, Engel J Jr. 2002. Interictal high-frequency oscillations (80–500 Hz) in the human epileptic brain: entorhinal cortex. Ann Neurol. 52:407–415.

Brown JA, Ramikie TS, Schmidt MJ, Baldi R, Garbett K, Everheart MG, Warren LE, Gellert L, Horvath S, Patel S, et al. 2015. Inhibition of parvalbumin-expressing interneurons results in complex behavioral changes. Mol Psychiatry. 12:1499–1507.

Buzsaki G. 1989. Two-stage model of memory trace formation: a role for "noisy" brain states. Neuroscience. 31:551–570.

Buzsaki G, Horvath Z, Urioste R, Hetke J, Wise K. 1992. High-frequency network oscillation in the hippocampus. Science. 256:1025–1027.

Buzsaki G, Moser EI. 2013. Memory, navigation and theta rhythm in the hippocampal-entorhinal system. Nat Neurosci. 16:130–138.

Caballero A, Diah KC, Tseng KY. 2013. Region-specific upregulation of parvalbumin-, but not calretinin-positive cells in the ventral hippocampus during adolescence. Hippocampus. 23:1331–1336.

Casanova E, Fehsenfeld S, Mantamadiotis T, Lemberger T, Greiner E, Stewart AF, Schütz G. 2001. A CamKIIalpha iCre BAC allows brain-specific gene inactivation. Genesis. 31:37–42.

Chrobak JJ, Buzsaki G. 1996. High-frequency oscillations in the output networks of the hippocampal-entorhinal axis of the freely behaving rat. J Neurosci. 16:3056–3066.

Courtin J, Chaudun F, Rozeske RR, Karalis N, Gonzalez-Campo C, Wurtz H, Abdi A, Baufreton J, Bienvenu TC, Herry C. 2014.

Prefrontal parvalbumin interneurons shape neuronal activity to drive fear expression. Nature. 505:92–96.
Csicsvari J, Hirase H, Czurko A, Mamiya A, Buzsaki G. 1999. Fast network oscillations in the hippocampal CA1 region of the behaving rat. J Neurosci. 19:RC20.
Csicsvari J, Hirase H, Mamiya A, Buzsaki G. 2000. Ensemble patterns of hippocampal CA3-CA1 neurons during sharp wave-associated population events. Neuron. 28:585–594.
Currie S, Heathfield KW, Henson RA, Scott DF. 1971. Clinical course and prognosis of temporal lobe epilepsy. A survey of 666 patients. Brain. 94:173–190.
Czeh B, Varga ZK, Henningsen K, Kovacs GL, Miseta A, Wiborg O. 2015. Chronic stress reduces the number of GABAergic interneurons in the adult rat hippocampus, dorsal-ventral and region-specific differences. Hippocampus. 25:393–405.
de la Fuente V, Freudenthal R, Romano A. 2011. Reconsolidation or extinction: transcription factor switch in the determination of memory course after retrieval. J Neurosci. 31:5562–5573.
Debiec J, LeDoux JE, Nader K. 2002. Cellular and systems reconsolidation in the hippocampus. Neuron. 36:527–538.
Donato F, Chowdhury A, Lahr M, Caroni P. 2015. Early- and late-born parvalbumin basket cell subpopulations exhibiting distinct regulation and roles in learning. Neuron. 85:770–786.
Donato F, Rompani SB, Caroni P. 2013. Parvalbumin-expressing basket-cell network plasticity induced by experience regulates adult learning. Nature. 504:272–276.
Dougherty KA, Islam T, Johnston D. 2012. Intrinsic excitability of CA1 pyramidal neurones from the rat dorsal and ventral hippocampus. J Physiol. 590:5707–5722.
Eichler SA, Förstera B, Smolinsky B, Juttner R, Lehmann TN, Fahling M, Schwarz G, Legendre P, Meier JC. 2009. Splice-specific roles of glycine receptor α3 in the hippocampus. Eur J Neurosci. 30:1077–1091.
Eichler SA, Kirischuk S, Jüttner R, Schäfermeier PK, Legendre P, Lehmann TN, Gloveli T, Grantyn R, Meier JC. 2008. Glycinergic tonic inhibition of hippocampal neurons with depolarising GABAergic transmission elicits histopathological signs of temporal lobe epilepsy. J Cell Mol Med. 12:2848–2866.
Eisenberg M, Kobilo T, Berman DE, Dudai Y. 2003. Stability of retrieved memory: inverse correlation with trace dominance. Science. 301:1102–1104.
Eschenko O, Ramadan W, Molle M, Born J, Sara SJ. 2008. Sustained increase in hippocampal sharp-wave ripple activity during slow-wave sleep after learning. Learn Mem. 15:222–228.
Girardeau G, Benchenane K, Wiener SI, Buzsaki G, Zugaro MB. 2009. Selective suppression of hippocampal ripples impairs spatial memory. Nat Neurosci. 12:1222–1223.
Golub Y, Mauch CP, Dahlhoff M, Wotjak CT. 2009. Consequences of extinction training on associative and non-associative fear in a mouse model of Posttraumatic Stress Disorder (PTSD). Behav Brain Res. 205:544–549.
Gulyas AI, Szabo GG, Ulbert I, Holderith N, Monyer H, Erdelyi F, Szabo G, Freund TF, Hajos N. 2010. Parvalbumin-containing fast-spiking basket cells generate the field potential oscillations induced by cholinergic receptor activation in the hippocampus. J Neurosci. 30:15134–15145.
Hajos N, Karlocai MR, Nemeth B, Ulbert I, Monyer H, Szabo G, Erdelyi F, Freund TF, Gulyas AI. 2013. Input-output features of anatomically identified CA3 neurons during hippocampal sharp wave/ripple oscillation in vitro. J Neurosci. 33: 11677–11691.
Hamilton DA, Brigman JL. 2015. Behavioral flexibility in rats and mice: contributions of distinct frontocortical regions. Genes Brain Behav. 14:4–21.
Hu H, Gan J, Jonas P. 2014. Interneurons. Fast-spiking, parvalbumin(+) GABAergic interneurons: from cellular design to microcircuit function. Science. 345:1255263.
Kanak DJ, Rose GM, Zaveri HP, Patrylo PR. 2013. Altered network timing in the CA3-CA1 circuit of hippocampal slices from aged mice. PLoS ONE. 8:e61364.
Kirwan CB, Wixted JT, Squire LR. 2008. Activity in the medial temporal lobe predicts memory strength, whereas activity in the prefrontal cortex predicts recollection. J Neurosci. 28:10541–10548.
Kranig SA, Duhme N, Waldeck C, Draguhn A, Reichinnek S, Both M. 2013. Different functions of hyperpolarization-activated cation channels for hippocampal sharp waves and ripples in vitro. Neurosci. 228:325–333.
Kubota H, Alle H, Betz H, Geiger JR. 2010. Presynaptic glycine receptors on hippocampal mossy fibers. Biochem Biophys Res Commun. 393:587–591.
Kudrimoti HS, Barnes CA, McNaughton BL. 1999. Reactivation of hippocampal cell assemblies: effects of behavioral state, experience, and EEG dynamics. J Neurosci. 19:4090–4101.
Laube B, Kuhse J, Betz H. 2000. Kinetic and mutational analysis of Zn2+ modulation of recombinant human inhibitory glycine receptors. J Physiol. 522:215–230.
Laxmi TR, Stork O, Pape HC. 2003. Generalisation of conditioned fear and its behavioural expression in mice. Behav Brain Res. 145:89–98.
Lee EA, Cho JH, Choi IS, Nakamura M, Park HM, Lee JJ, Lee MG, Choi BJ, Jang IS. 2009. Presynaptic glycine receptors facilitate spontaneous glutamate release onto hilar neurons in the rat hippocampus. J Neurochem. 109:275–286.
Legendre P, Förstera B, Jüttner R, Meier JC. 2009. Glycine receptors caught between genome and proteome - Functional implications of RNA editing and splicing. Front Mol Neurosci. 2:23.
Lesting J, Geiger M, Narayanan RT, Pape HC, Seidenbecher T. 2011. Impaired extinction of fear and maintained amygdala-hippocampal theta synchrony in a mouse model of temporal lobe epilepsy. Epilepsia. 52:337–346.
Maier N, Morris G, Schuchmann S, Korotkova T, Ponomarenko A, Bohm C, Wozny C, Schmitz D. 2014. Dendritic inhibition in the hippocampus supports fear learning. Science. 343:857–863.
Lu CB, Jefferys JG, Toescu EC, Vreugdenhil M. 2011. In vitro hippocampal gamma oscillation power as an index of in vivo CA3 gamma oscillation strength and spatial reference memory. Neurobiol Learn Mem. 95:221–230.
Maggio N, Segal M. 2009. Differential modulation of long-term depression by acute stress in the rat dorsal and ventral hippocampus. J Neurosci. 29:8633–8638.
Maggio N, Segal M. 2007. Striking variations in corticosteroid modulation of long-term potentiation along the septotemporal axis of the hippocampus. J Neurosci. 27:5757–5765.
Maier N, Morris G, Johenning FW, Schmitz D. 2009. An approach for reliably investigating hippocampal sharp wave-ripples in vitro. PLoS ONE. 4:e6925.
Maier N, Morris G, Schuchmann S, Korotkova T, Ponomarenko A, Bohm C, Wozny C, Schmitz D. 2012. Cannabinoids disrupt hippocampal sharp wave-ripples via inhibition of glutamate release. Hippocampus. 22:1350–1362.
Maier N, Nimmrich V, Draguhn A. 2003. Cellular and network mechanisms underlying spontaneous sharp wave-ripple complexes in mouse hippocampal slices. J Physiol. 550:873–887.
Mamiya N, Fukushima H, Suzuki A, Matsuyama Z, Homma S, Frankland PW, Kida S. 2009. Brain region-specific gene expression activation required for reconsolidation and extinction of contextual fear memory. J Neurosci. 29:402–413.

Marshall L, Helgadottir H, Molle M, Born J. 2006. Boosting slow oscillations during sleep potentiates memory. Nature. 444:610–613.

McCracken LM, Trudell JR, McCracken ML, Harris RA. 2013. Zinc-Dependent Modulation of alpha2- and alpha3-Glycine Receptor Subunits by Ethanol. Alcohol Clin Exp Res. 37:2002–2010.

McEwen BS. 2012. Brain on stress: how the social environment gets under the skin. Proc Natl Acad Sci USA. 109:17180–17185.

Milad MR, Quirk GJ. 2002. Neurons in medial prefrontal cortex signal memory for fear extinction. Nature. 420:70–74.

Miles R, Toth K, Gulyas AI, Hajos N, Freund TF. 1996. Differences between somatic and dendritic inhibition in the hippocampus. Neuron. 16:815–823.

Myers KM, Davis M. 2007. Mechanisms of fear extinction. Mol Psychiatry. 12:120–150.

Nadasdy Z, Hirase H, Czurko A, Csicsvari J, Buzsaki G. 1999. Replay and time compression of recurring spike sequences in the hippocampus. J Neurosci. 19:9497–9507.

Nader K, Schafe GE, Le Doux JE. 2000. Fear memories require protein synthesis in the amygdala for reconsolidation after retrieval. Nature. 406:722–726.

Nakashiba T, Buhl DL, McHugh TJ, Tonegawa S. 2009. Hippocampal CA3 output is crucial for ripple-associated reactivation and consolidation of memory. Neuron. 62:781–787.

Olsen RH, Marzulla T, Raber J. 2014. Impairment in extinction of contextual and cued fear following post-training whole-body irradiation. Front Behav Neurosci. 8:231.

Papatheodoropoulos C, Kostopoulos G. 2000. Dorsal-ventral differentiation of short-term synaptic plasticity in rat CA1 hippocampal region. Neurosci Lett. 286:57–60.

Papatheodoropoulos C, Kostopoulos G. 2002. Spontaneous, low frequency (approximately 2–3 Hz) field activity generated in rat ventral hippocampal slices perfused with normal medium. Brain Res Bull. 57:187–193.

Parsons RG, Ressler KJ. 2013. Implications of memory modulation for post-traumatic stress and fear disorders. Nat Neurosci. 16:146–153.

Pilly PK, Grossberg S. 2012. How do spatial learning and memory occur in the brain? Coordinated learning of entorhinal grid cells and hippocampal place cells. J Cogn Neurosci. 24:1031–1054.

Pinna G, Rasmusson AM. 2014. Ganaxolone improves behavioral deficits in a mouse model of post-traumatic stress disorder. Front Cell Neurosci. 8:256.

Prasad JA, Chudasama Y. 2013. Viral tracing identifies parallel disynaptic pathways to the hippocampus. J Neurosci. 33: 8494–8503.

Rasch B, Buchel C, Gais S, Born J. 2007. Odor cues during slow-wave sleep prompt declarative memory consolidation. Science. 315:1426–1429.

Rosas-Vidal LE, Do-Monte FH, Sotres-Bayon F, Quirk GJ. 2014. Hippocampal–prefrontal BDNF and memory for fear extinction. Neuropsychopharmacology. 39:2161–2169.

Rozeske RR, Valerio S, Chaudun F, Herry C. 2015. Prefrontal neuronal circuits of contextual fear conditioning. Genes Brain Behav. 14:22–36.

Rudy JW, Matus-Amat P. 2005. The ventral hippocampus supports a memory representation of context and contextual fear conditioning: implications for a unitary function of the hippocampus. Behav Neurosci. 119:154–163.

Ruediger S, Vittori C, Bednarek E, Genoud C, Strata P, Sacchetti B, Caroni P. 2011. Learning-related feedforward inhibitory connectivity growth required for memory precision. Nature. 473:514–518.

Sangha S, Narayanan RT, Bergado-Acosta JR, Stork O, Seidenbecher T, Pape HC. 2009. Deficiency of the 65 kDa isoform of glutamic acid decarboxylase impairs extinction of cued but not contextual fear memory. J Neurosci. 29:15713–15720.

Schlingloff D, Kali S, Freund TF, Hajos N, Gulyas AI. 2014. Mechanisms of sharp wave initiation and ripple generation. J Neurosci. 20:11385–11398.

Shrager Y, Kirwan CB, Squire LR. 2008. Activity in both hippocampus and perirhinal cortex predicts the memory strength of subsequently remembered information. Neuron. 59: 547–553.

Sparta DR, Hovelso N, Mason AO, Kantak PA, Ung RL, Decot HK, Stuber GD. 2014. Activation of prefrontal cortical parvalbumin interneurons facilitates extinction of reward-seeking behavior. J Neurosci. 34:3699–3705.

Stark E, Roux L, Eichler R, Senzai Y, Royer S, Buzsaki G. 2014. Pyramidal cell-interneuron interactions underlie hippocampal ripple oscillations. Neuron. 83:467–480.

Steullet P, Cabungcal JH, Kulak A, Kraftsik R, Chen Y, Dalton TP, Cuenod M, Do KQ. 2010. Redox dysregulation affects the ventral but not dorsal hippocampus: impairment of parvalbumin neurons, gamma oscillations, and related behaviors. J Neurosci. 30:2547–2558.

Suzuki SS, Smith GK. 1988. Spontaneous EEG spikes in the normal hippocampus. II. Relations to synchronous burst discharges. Electroencephalogr Clin Neurophysiol. 69:532–540.

VanElzakker MB, Dahlgren MK, Davis FC, Dubois S, Shin LM. 2014. From Pavlov to PTSD: the extinction of conditioned fear in rodents, humans, and anxiety disorders. Neurobiol Learn Mem. 113:3–18.

Vazquez B, Devinsky O. 2003. Epilepsy and anxiety. Epilepsy Behav. (Suppl 4):S20–S25.

Wilson MA, McNaughton BL. 1994. Reactivation of hippocampal ensemble memories during sleep. Science. 265:676–679.

Winkelmann A, Maggio N, Eller J, Caliskan G, Semtner M, Häussler U, Jüttner R, Dugladze T, Smolinsky B, Kowalczyk S, et al. 2014. Changes in neural network homeostasis trigger neuropsychiatric symptoms. J Clin Invest. 124:696–711.

Zeitlin R, Patel S, Solomon R, Tran J, Weeber EJ, Echeverria V. 2012. Cotinine enhances the extinction of contextual fear memory and reduces anxiety after fear conditioning. Behav Brain Res. 228:284–293.

Zhu H, Pleil KE, Urban DJ, Moy SS, Kash TL, Roth BL. 2014. Chemogenetic inactivation of ventral hippocampal glutamatergic neurons disrupts consolidation of contextual fear memory. Neuropsychopharmacology. 39:1880–1892.